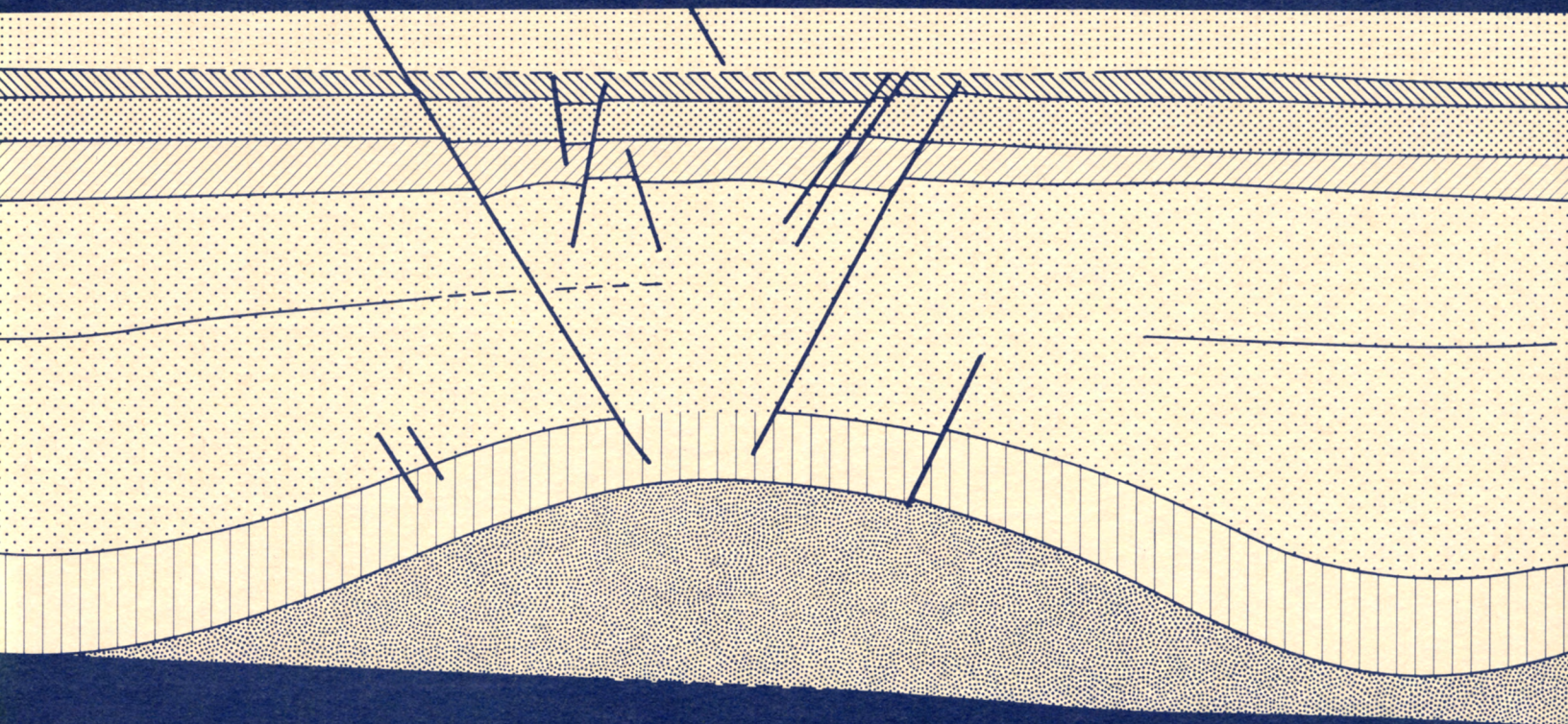


Geological Circular 82-4

# ***Fault Tectonics of the East Texas Basin***

M. P. A. Jackson

**Bureau of Economic Geology • W. L. Fisher, Director**  
*The University of Texas at Austin • Austin, Texas*



1982



Geological Circular 82-4

FAULT TECTONICS OF THE EAST TEXAS BASIN

by

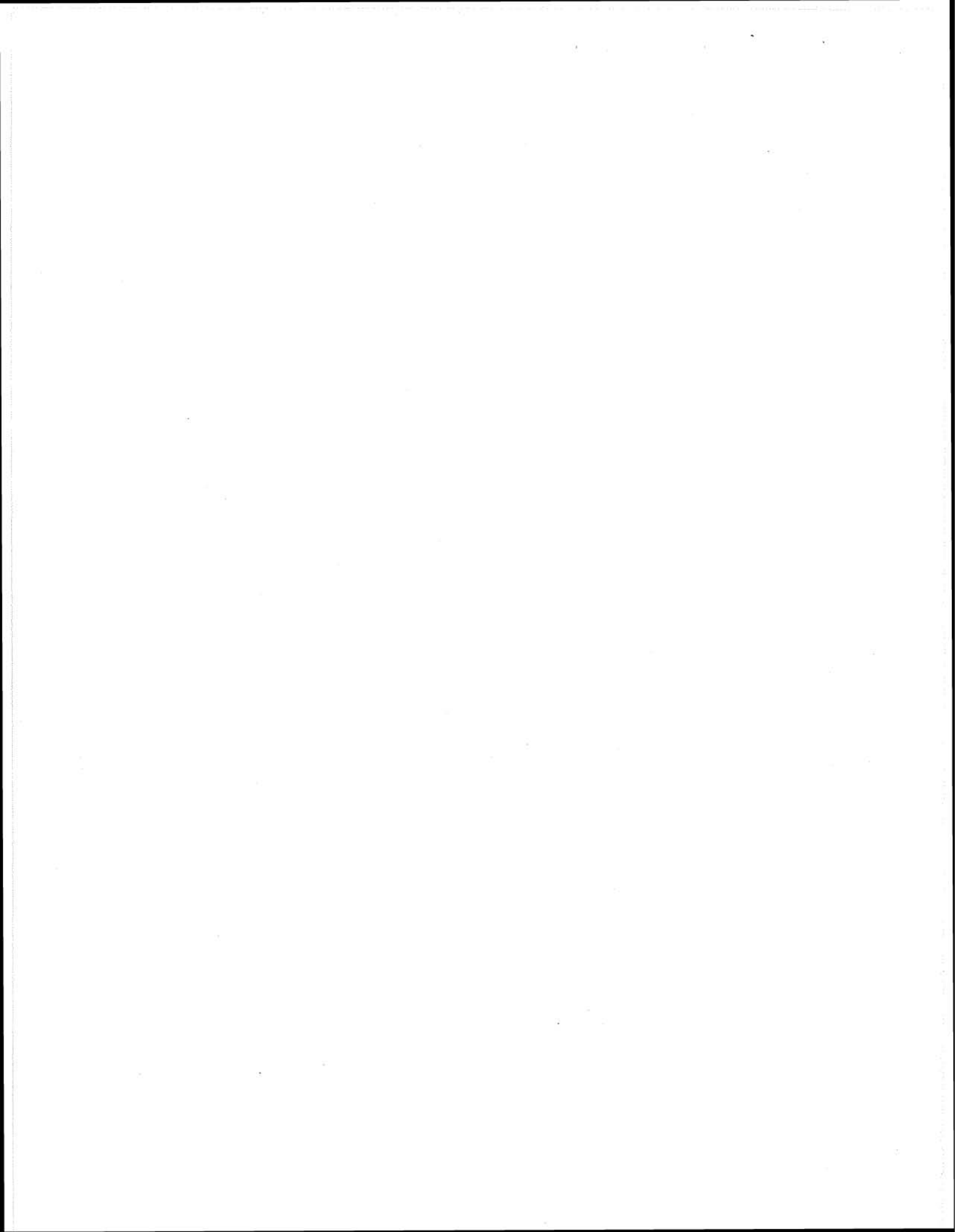
M. P. A. Jackson

assisted by B. D. Wilson

Funding provided by the U.S. Department of Energy  
under Contract No. DE-AC97-80ET-46617

Bureau of Economic Geology  
W. L. Fisher, Director  
The University of Texas at Austin  
Austin, Texas

1982



## CONTENTS

	Page
Abstract . . . . .	1
Introduction . . . . .	1
Structural framework . . . . .	1
Mexia-Talco Fault Zone . . . . .	4
Faults in the central basin . . . . .	17
Elkhart Graben . . . . .	18
Mount Enterprise Fault Zone . . . . .	23
Seismic potential of East Texas faults . . . . .	27
Conclusions . . . . .	28
Acknowledgments . . . . .	28
References . . . . .	29

## Figures

1. Stratigraphic column of the East Texas Basin . . . . .	2
2. Regional tectonic setting of the East Texas Basin . . . . .	3
3. Structural cross sections across the East Texas Basin . . . . .	5
4. Map of the East Texas salt-diapir and salt-pillow provinces . . . . .	6
5. Surface fault traces in the East Texas Basin . . . . .	7
6. Fault traces on horizon 1 and their relation to salt diapirs, salt pillows, and turtle structures . . . . .	8
7. Fault traces on horizon 2 and their relation to salt diapirs, salt pillows, and turtle structures . . . . .	9
8. Fault traces on horizon 3 and their relation to salt diapirs, salt pillows, and turtle structures . . . . .	10
9. Cross section of Mexia Fault Zone based on well logs . . . . .	11
10. Interpretation of a seismic profile across the northern part of the Mexia Fault Zone . . . . .	12
11. Time-to-depth converted seismic section of Mexia Fault Zone . . . . .	13
12. Bar graphs of throws inferred from structure-contour maps of the Mexia-Talco Fault Zone . . . . .	15

13. Conceptual diagram of a symmetric graben formed by asymmetric extension . . . . .	17
14. Time-to-depth converted seismic section across the junction of Van and Ash Salt Pillows . . . . .	19
15. Map of fault traces of Elkhart-Mount Enterprise Fault Zone on horizon 2 showing relation to salt pillows, turtle structures, regional dip, and adjacent faults . . . . .	20
16. Bar graphs of throws of the Elkhart-Mount Enterprise Fault Zone inferred from structure-contour maps on horizon 1 . . . . .	21
17. Bar graphs of throws of the Elkhart-Mount Enterprise Fault Zone inferred from structure-contour maps on horizon 2 . . . . .	22
18. Time-to-depth converted seismic section across the central part of the Mount Enterprise Fault Zone . . . . .	24
19. Time-to-depth converted seismic section across the western part of the Mount Enterprise Fault Zone . . . . .	26

## ABSTRACT

Principal fault systems in the East Texas Basin were examined in terms of their distribution, geometry, displacement history, and possible origins. All the faults studied are normal and moved syndepositionally over approximately 120 Ma (million years); some have listric shapes and associated rollover anticlines. The faults formed by processes associated with gravitationally induced creep of the Louann Salt, such as gliding over a salt décollement zone, crestal extension and collapse over salt pillows and turtle structures, and salt withdrawal from beneath downthrown blocks. None of the fault zones were caused by marginal flexure of the basins or salt diapirism; there is little evidence of basement control. Paucity of data prevents a reliable interpretation of the Mount Enterprise Fault, but our data suggest that none of the fault zones in this basin pose a seismic threat to a hypothetical nuclear-waste repository in the Gulf Coast area.

## INTRODUCTION

Safe containment of high-level nuclear wastes in geologic formations requires that wastes be isolated in an environment free from risk of severe earthquakes. This study examines the distribution, geometry, displacement history, and possible origins of the principal fault systems of the East Texas Basin to assess the risk of seismic shock to a potential nuclear-waste repository in the Gulf Coast area. Radial faults over diapirs are not discussed in this paper because of their small size, local distribution, and obvious relation to diapiric creep of salt. In this report the reader is assumed to be familiar with the stratigraphy of the East Texas Basin, as summarized in figure 1.

## STRUCTURAL FRAMEWORK

A map of the tectonic setting of the East Texas Basin (fig. 2) reveals that the western and northern margins of the basin coincide with other geologic structures varying from Pennsylvanian to Tertiary age. The Pennsylvanian Ouachita fold and thrust belt crops out in Arkansas and Oklahoma and extends to southwest Texas beneath Mesozoic cover (Thomas, 1976). Stratal shortening of Ouachita marine deposits generated northwest-verging folds and thrusts. Early Mesozoic continental rifting of this Paleozoic terrane can be inferred from the confinement of the Triassic Eagle Mills rift clastics to

ERA-THEM	SYSTEM	SERIES	GROUP	FORMATION
CENOZOIC	TERTIARY	EOCENE	CLAIBORNE	YEGUA
				COOK MOUNTAIN
				SPARTA
				WECHES
				QUEEN CITY
		REKLAW		
		GARRIZO		
		PALEOCENE	WILCOX	UNDIFFERENTIATED
				MIDWAY
		MESOZOIC	CRETACEOUS	UPPER CRETACEOUS
UPPER NAVARRO MARL				
NACATOCH SAND				
LOWER NAVARRO				
UPPER TAYLOR				
TAYLOR	PECAN GAP CHALK			
	WOLFE CITY SAND			
	LOWER TAYLOR			
AUSTIN	GOBER CHALK			
	BROWNSTOWN			
	BLOSSOM SAND			
	BONHAM CLAY			
	Glaucolithic Chalk Stringer			
AUSTIN CHALK				
EAGLE FORD	Sub Clarksville Mbr.			
	EAGLE			
	FORD			
WOODBINE	WOODBINE			
	Lewisville Mbr. Dexter Sand Mbr.			
WASHITA	MANESS SHALE			
	BUDA LIMESTONE			
	GRAYSON SHALE			
	MAIN STREET LIMESTONE			
	WENO-PAW PAW LIMESTONE			
	DENTON SHALE			
	FORT WORTH LIMESTONE			
	DUCK CREEK SHALE			
	DUCK CREEK LIMESTONE			
	KIAMICHI SHALE			
FREDERICKSBURG	GOODLAND LIMESTONE			
	PALUXY			
LOWER CRETACEOUS	TRINITY	UPPER GLEN ROSE		
		MASSIVE ANHYDRITE		
		Rodessa Member		
		James Limestone Mbr.		
		Pine Island Shale Member		
	Petter (Sligo) Member			
	TRAVIS PEAK (HOSSTON)	TRAVIS PEAK (HOSSTON)		
		COTTON VALLEY	SCHULER	
			BOSSIER	
			GILMER LIMESTONE (COTTON VALLEY LIMESTONE)	
LOUARK		BUCKNER		
	SMACKOVER			
MIDDLE JURASSIC	LOUANN	NORPHLET		
		LOUANN SALT		
		WERNER		
Upper Triassic	EAGLE MILLS			
PALEOZOIC		OUACHITA		

Figure 1. Stratigraphic column of the East Texas Basin. Horizons 1 through 3 (arrows) refer to horizons selected for subsurface fault maps (figs. 6-8) (after Wood and Guevara, 1981).

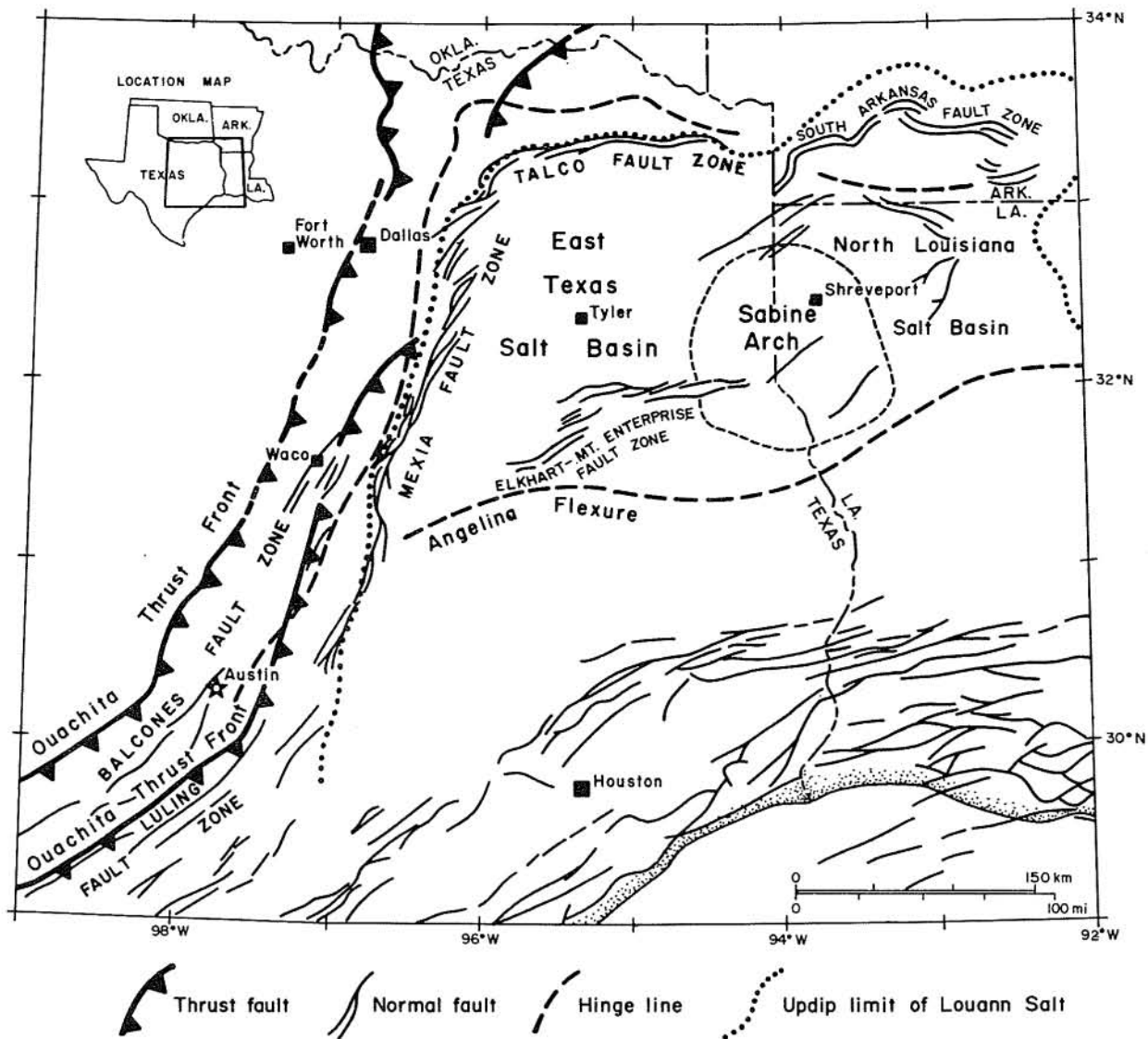


Figure 2. Regional tectonic setting of the East Texas Basin. Position of Angolina Flexure is mapped at base of Austin Chalk. Adapted from Martin (1978).

grabens and half grabens parallel to the Ouachita trends (Salvador and Green, 1980). Further subsidence allowed marine incursions that deposited the evaporitic Louann Salt on an eroded post-rift, pre-breakup terrane. The updip limit of the Louann Salt (fig. 2) is also parallel to the Ouachita trends, which indicates that during the Jurassic the Ouachita area was still elevated with respect to the subsiding East Texas Basin. A poorly defined monoclinial hinge line is present updip of the Louann Salt (fig. 2), but is too weak to delineate the western and northern margins of the basin. This part of the basin margin is therefore defined by the Mexia-Talco Fault Zone, a peripheral graben system active from the Jurassic to the Eocene that coincides with the updip limit of the Louann Salt.



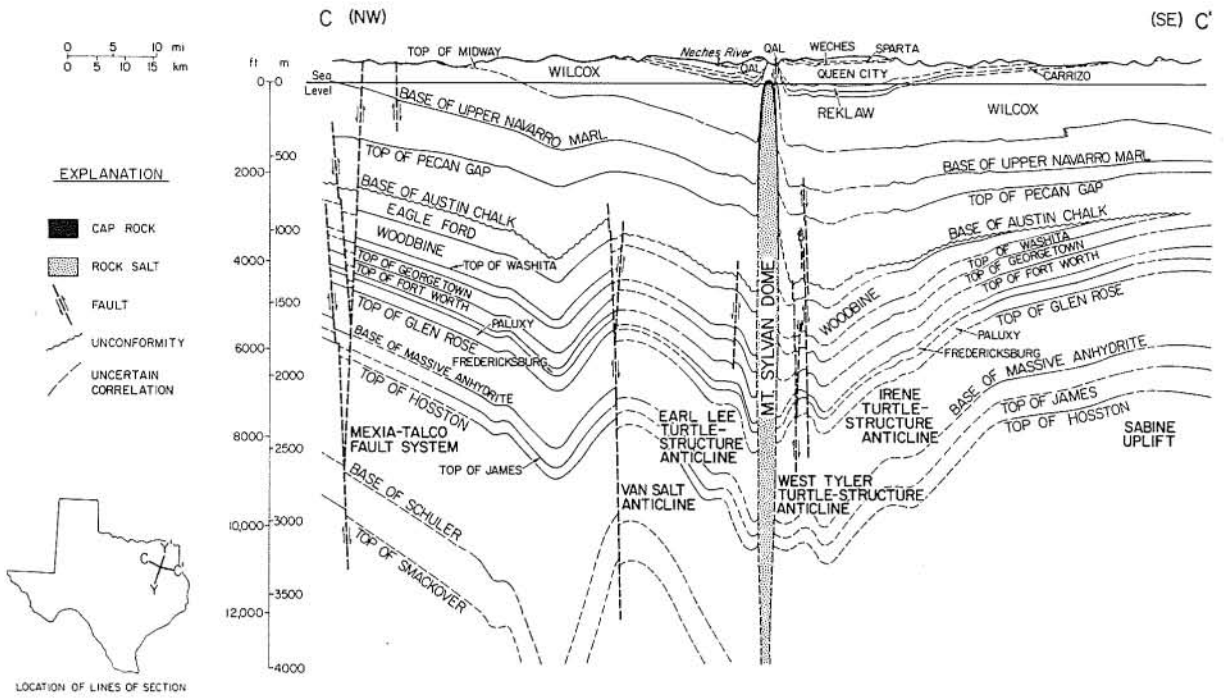
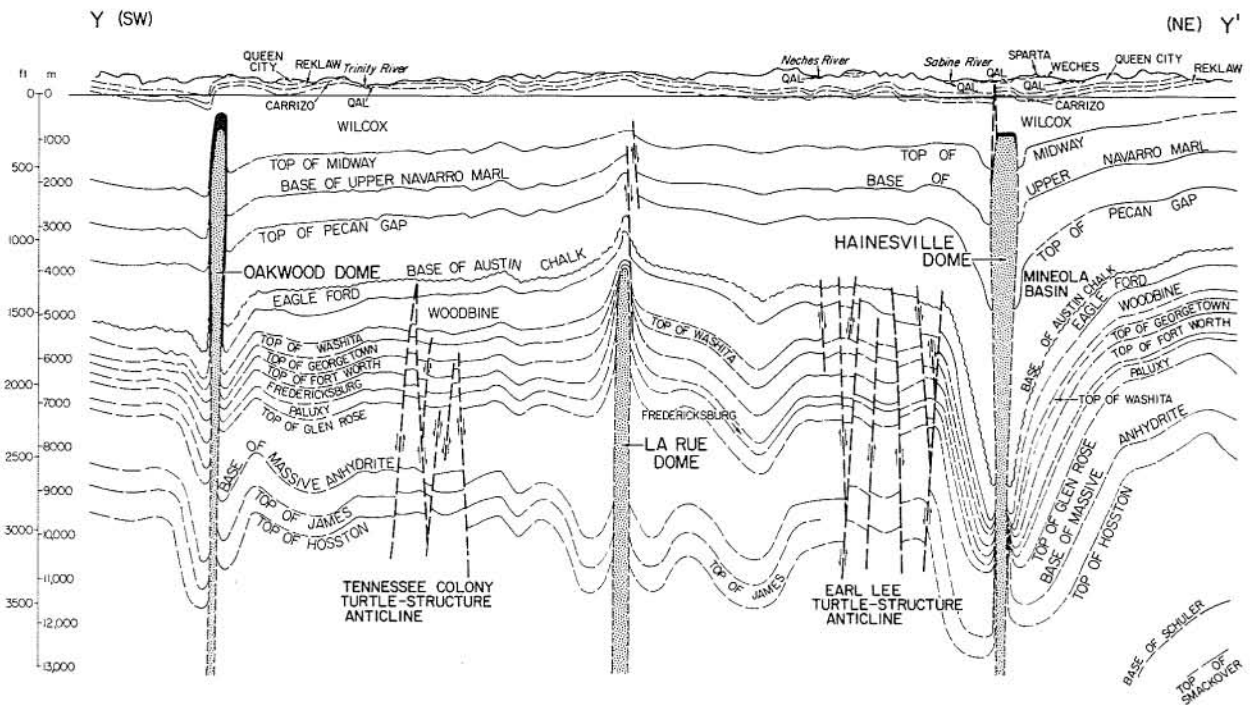
The Sabine Arch, a broad structural dome, forms the eastern margin of the basin. The southern margin of the basin is defined by the Angelina Flexure, a hinge line that is generally monoclinial at its ends and anticlinal in the middle. The Elkhart-Mount Enterprise Fault Zone extends from just north of the western end of the Angelina Flexure to the center of the Sabine Arch (fig. 2).

The gross structure of the East Texas Basin consists of regular basinward dips in the east, west, and north (fig. 3) and a low rim in the south along the Angelina Flexure. Deformation within the basin appears to be related solely to large-scale, gravitationally induced creep of salt (halokinesis). As a result of salt flow, the synclinal form of the East Texas Basin has been distorted by three types of second-order anticlinal structures: (1) salt pillows, which are large, low-amplitude upwarps cored by salt; (2) salt diapirs, which are subvertical, cylindrical salt stocks that have pierced the adjacent strata; and (3) turtle structures, which are salt-free growth anticlines formed not by arching of their crests but by subsidence of their flanks due to collapse of underlying salt pillows during salt diapirism (Trusheim, 1960). These three types of anticline are termed "salt-related structures." Their distribution is such that a peripheral zone of planar salt surrounds an irregular area of salt pillows which, in turn, surrounds salt diapirs in the center of the basin where the Louann Salt is thickest (fig. 4).

### MEXIA-TALCO FAULT ZONE

The Mexia and Talco Fault Zones are each defined by strike-parallel normal faults forming narrow grabens. These two zones of parallel faults are connected by a zone of en echelon normal faults, termed the "Great Bend," in Kaufman and Hunt Counties. Fault distributions at the surface and at three subsurface horizons (refer to fig. 1 for stratigraphic levels) are shown in figures 5 through 8.

The graben geometry of the Mexia Fault Zone is confirmed by a cross section, based on well-log data (fig. 9), illustrating a compound graben with multiple downthrows toward its center. However, well data are insufficient to define the three-dimensional shape of the fault system or to elucidate its origin. Seismic reflection profiles indicate that the graben is based in the wedgeout zone of the Louann Salt or, updip of this, in the base of the Smackover Formation (figs. 10 and 11). The Mexia Fault Zone overlies the boundary fault of a half graben containing Eagle Mills red beds (Jackson and Harris, 1981), which suggests that the location of the fault zone here was controlled partly by Triassic rift faults and partly by the updip limit of the Louann Salt. A more detailed view of the Mexia Fault Zone farther north, in the form of a time-to-depth converted seismic section



- EXPLANATION
- CAP ROCK
  - ▨ ROCK SALT
  - FAULT
  - - UNCONFORMITY
  - · - UNCERTAIN CORRELATION

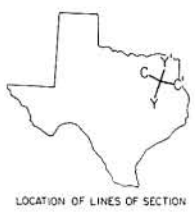


Figure 3. Structural cross sections across the East Texas Basin. After Wood and Guevara (1981).

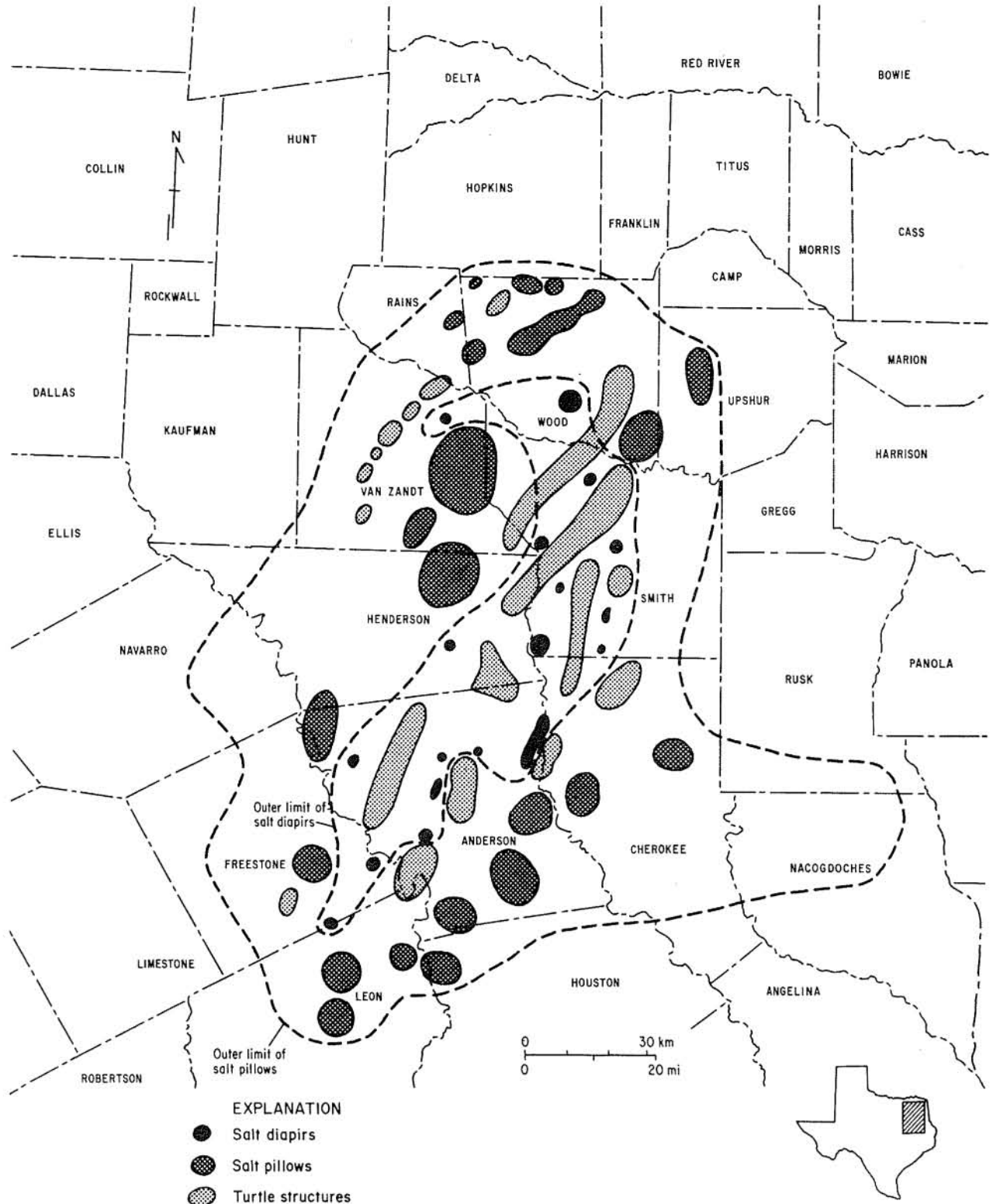


Figure 4. Map of the East Texas salt-diapir and salt-pillow provinces based on borehole and gravity data. Bulge to the southwest in Nacogdoches and Rusk Counties contains numerous small pillows not shown on map. Adapted from Wood (1981).

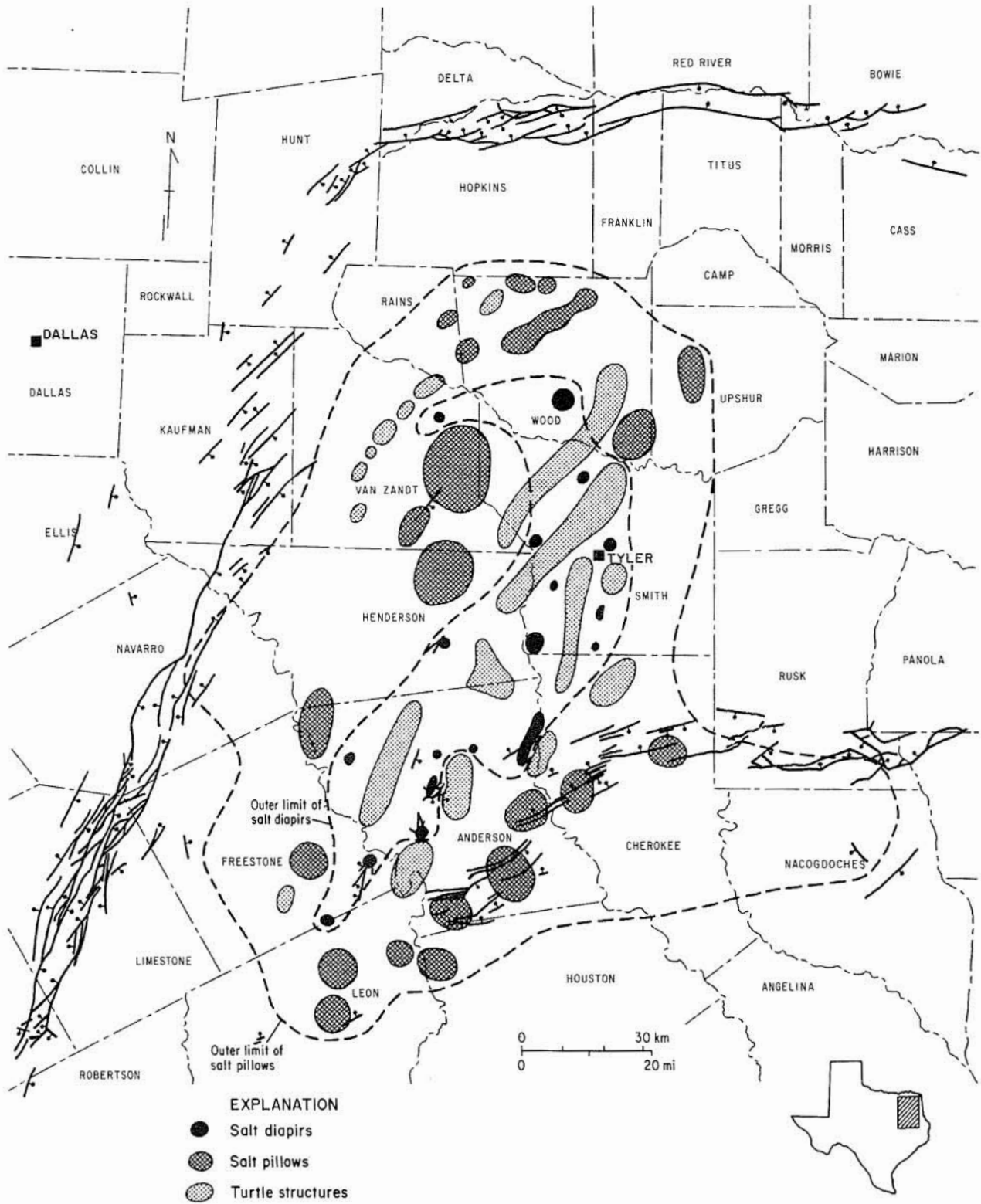


Figure 5. Surface fault traces in the East Texas Basin. After Barnes (1965, 1966, 1967, 1968, 1970, 1972).

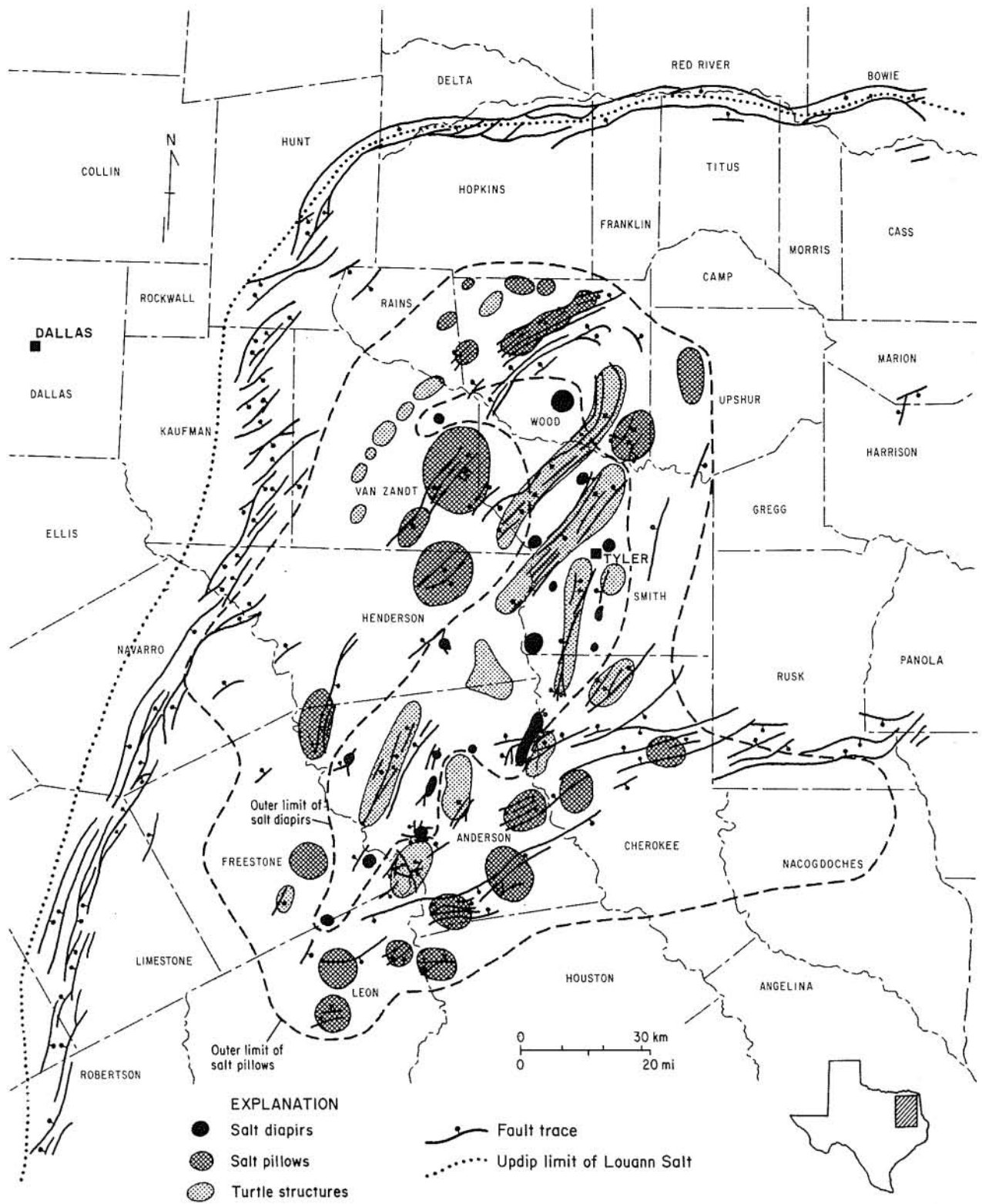


Figure 6. Fault traces on horizon 1 (base of Austin Chalk) and their relation to salt diapirs, salt pillows, and turtle structures. Fault traces from GEOMAP Company (1980).

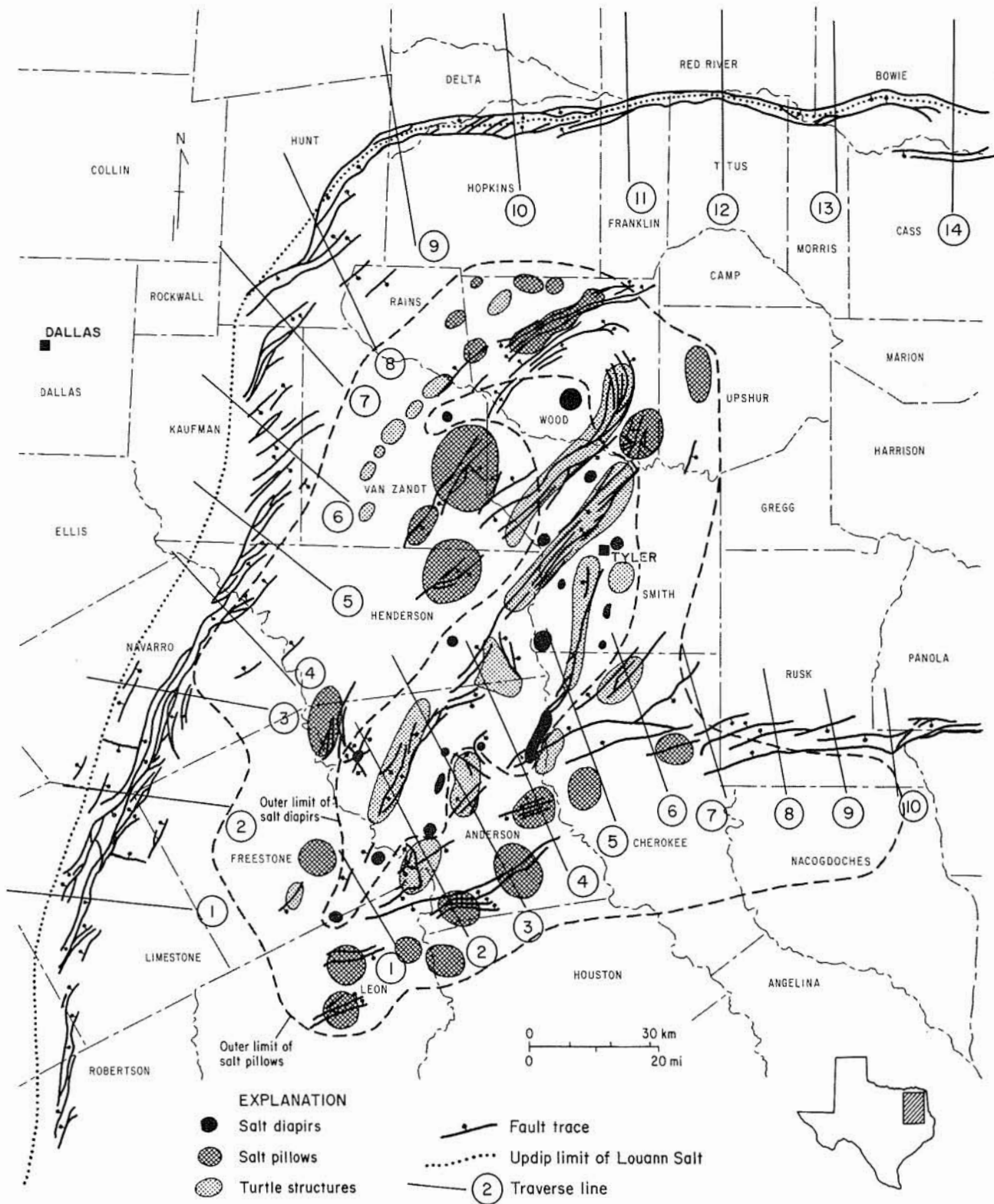


Figure 7. Fault traces on horizon 2 (top of Paluxy Formation, base of Massive Anhydrite, top of James Limestone, top of Pettet Limestone) and their relation to salt diapirs, salt pillows, and turtle structures. Fault traces from GEOMAP Company (1980).

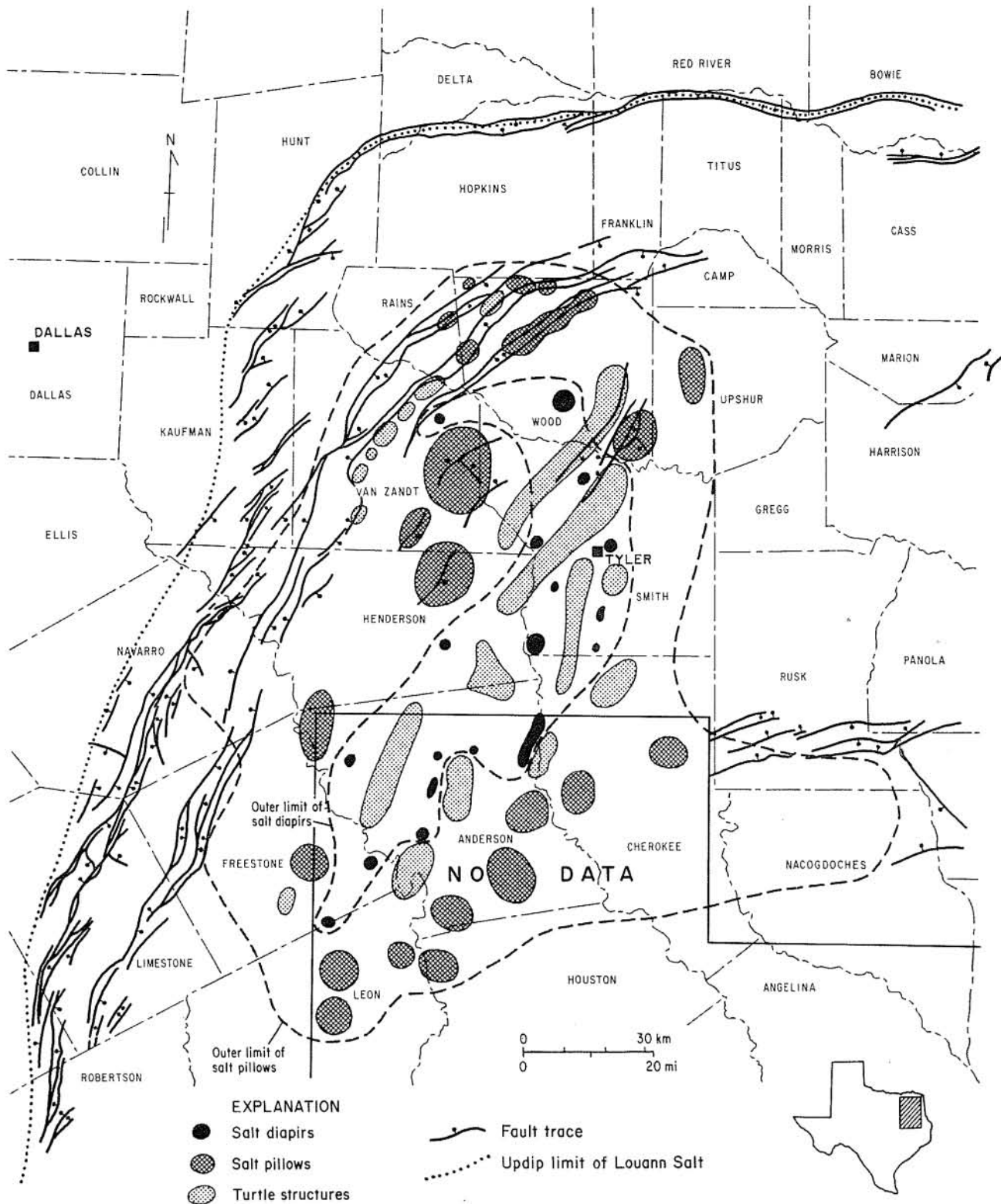
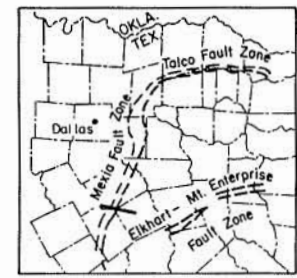
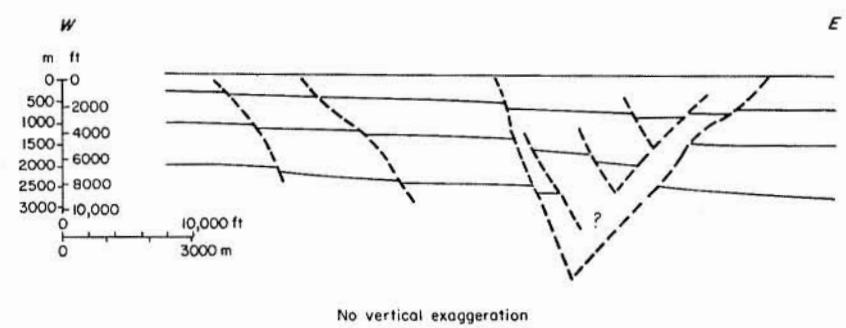
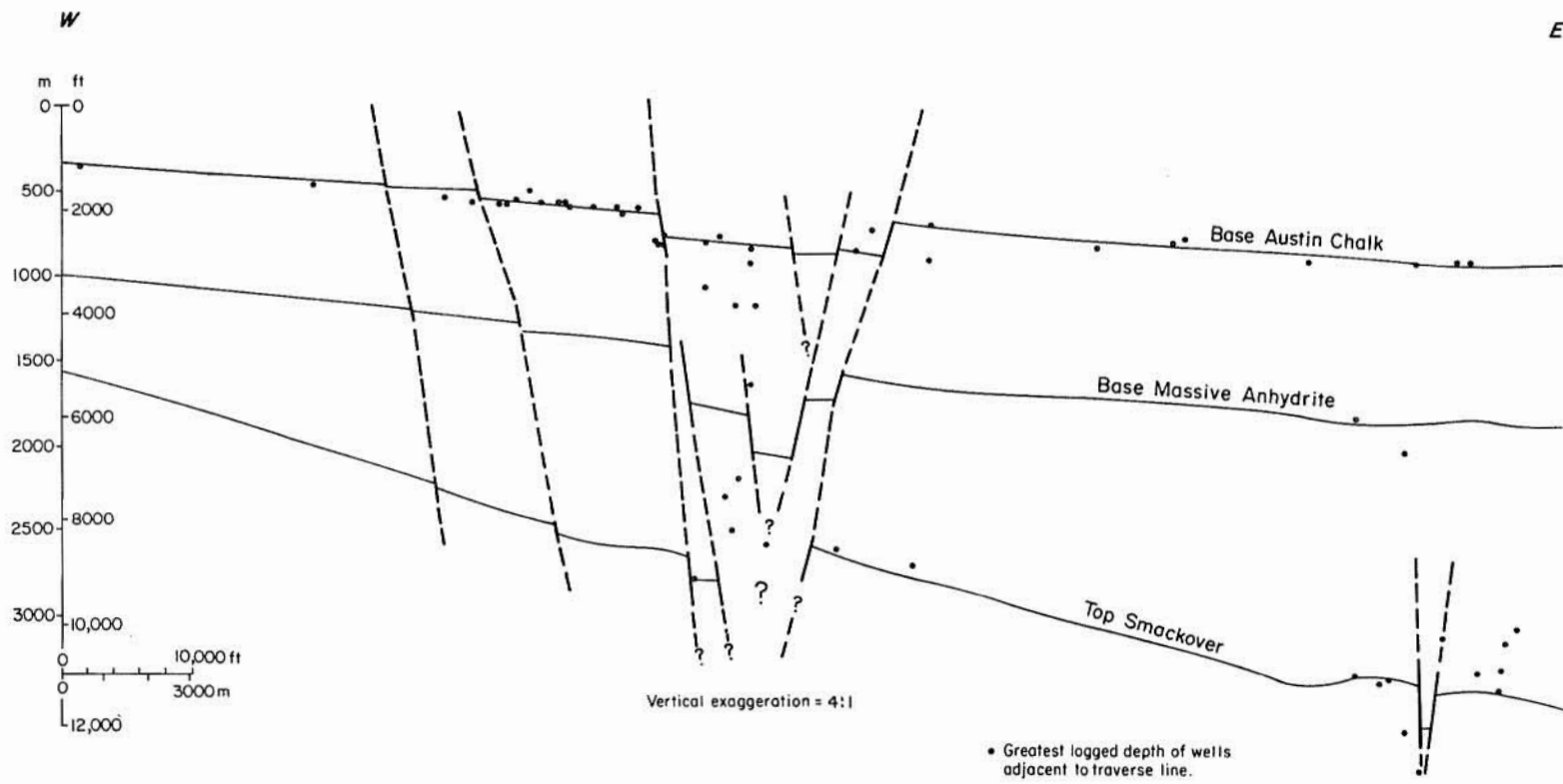


Figure 8. Fault traces on horizon 3 (base of "B" line, top of Gilmer Formation, top of Smackover Formation, top of Paleozoic basement) and their relation to salt diapirs, salt pillows, and turtle structures. Fault traces from GEOMAP Company (1980).



**Figure 9. Cross section of Mexia Fault Zone based on well logs (dots define base of wells). A graben defined by multiple faults interrupts the homoclinal basin margin.**



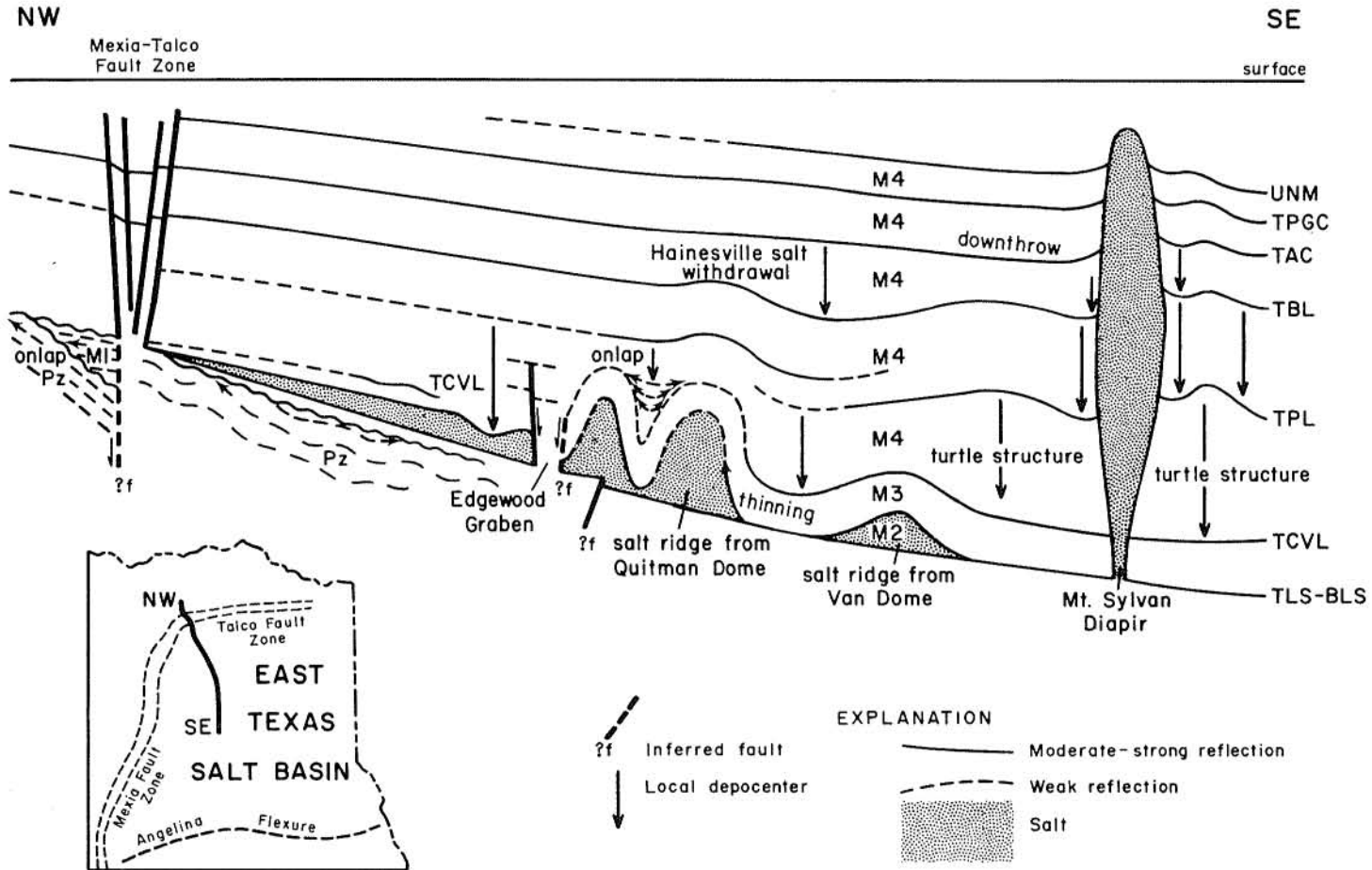
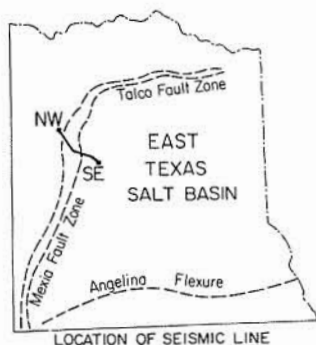
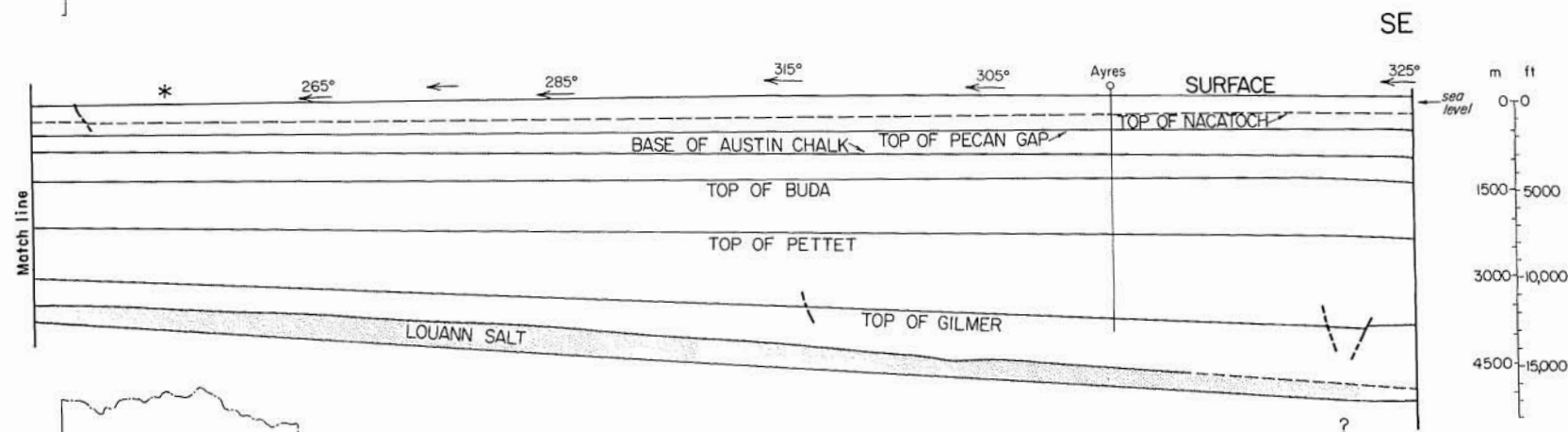
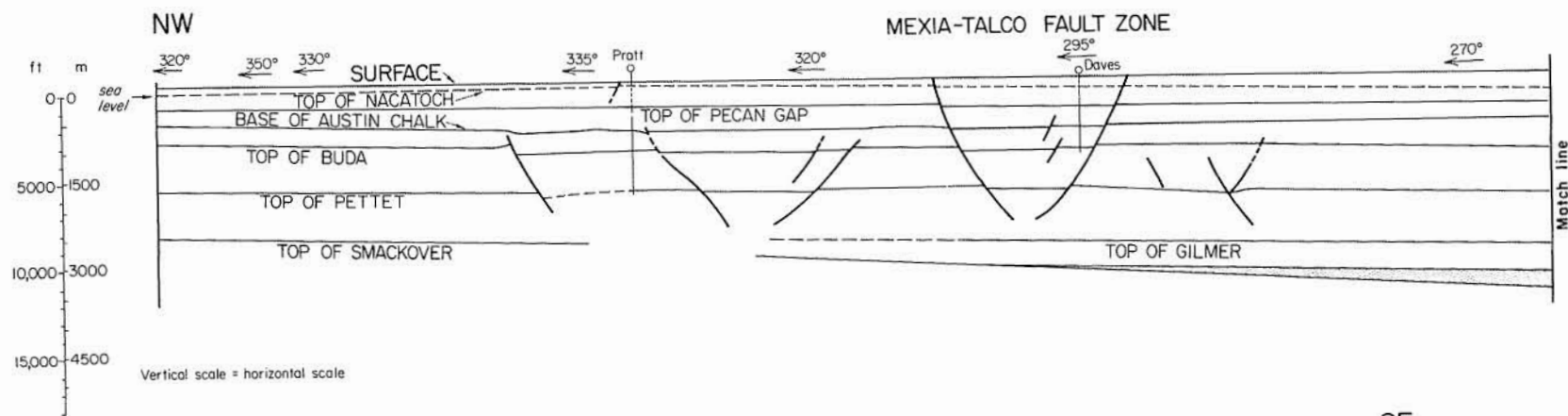


Figure 10. Interpretation (not to scale) of a seismic profile across the northern part of the Mexia Fault Zone showing tectonic characteristics of the peripheral graben and seismic stratigraphy. Eagle Mills clastics (seismic unit M1) are present in an Upper Triassic-Lower Jurassic half graben (confirmed by boreholes); the Mexia graben overlies this fault, indicating the possible influence of pre-Louann faulting on this part of the Mexia-Talco Fault Zone. The Louann Salt (seismic unit M2) pinches out updip beneath the Mexia graben and moves downdip into a series of salt pillows, whose growth began prior to Cotton Valley time. Seismic reflectors as follows: TLS-BLS, top and base of Louann Salt; TCVL, top of Gilmer Limestone; TPL, top of Pettet Limestone; TBL, top of Buda Limestone; TAC, top of Austin Chalk; TPGC, top of Pecan Gap Chalk; UNM, Upper Navarro Marl. Adapted from Jackson and Harris (1981).



- EXPLANATION**
- Reflector
  - - - Uncertain reflector
  - - - Fault trace
  - ♀ Well providing depth control
  - \* Seismic depth control
  - Louann Salt

- Errors in reflector depths**
- Nacatoch ± 90m (300 ft)
  - Pecan Gap ± 90m (300 ft)
  - Austin Chalk ± 90m (300 ft)
  - Buda ± 90m (300 ft)
  - Pettel ± 120m (400 ft)
  - Gilmer ± 180m (600 ft)
  - Louann ± 180m (600 ft)

Fault traces projected to surface on the basis of Barnes (1972)  
 Seismic picks by D.W. Harris and C.D. Winker  
 Time-to-depth conversion by R.E. Anderson and T.E. Ewing  
 based on electric logs and seismic velocity analyses.

**Figure 11. Time-to-depth converted seismic section of Mexia Fault Zone to scale. Note (1) lack of flexure in pre-Louann basement; (2) coincidence of fault zone with updip limit of Louann Salt; (3) increasing downward displacement toward ill-defined base of graben; (4) buried faults adjacent to Mexia graben that became inactive in the Middle Cretaceous.**

(fig. 11), illustrates several important features: (1) all the faults are homothetic<sup>1</sup> rather than antithetic, in that they increase the structural relief; (2) the pre-Louann basement is not flexed below the fault zone (nor in the other two seismic lines examined in this study); (3) the graben is symmetrical, and the fault traces are not strongly curved; (4) increasing throws downward indicate syndepositional faulting; (5) the basal strata in the central graben are missing, implying a mobile substratum such as shale or salt in the Cotton Valley-Hosston interval; and (6) the Louann Salt wedges out toward the base of the graben, where it is so thin that its top and bottom reflectors merge.

Throws on faults of this graben system were analyzed on 14 traverse lines spaced approximately 25 km apart and oriented normal to the strike of the grabens, thus parallel to dip slip (fig. 7). All downthrows are relative. The following parameters were used in the analysis:

Measured downthrow with translation of downthrown block to north or west toward platform =  $+d_i$ .

Measured downthrow with translation of downthrown block to south or east toward East Texas Basin =  $-d_i$ .

$$\text{North downthrows} = \sum_{i=1}^n +d_i$$

$$\text{South downthrows} = \sum_{i=1}^n -d_i$$

$$\text{Total downthrow} = \sum_{i=1}^n |d_i|$$

$$\text{Net downthrow} = \sum_{i=1}^n d_i = \left[ \sum_{i=1}^n +d_i \right] + \left[ \sum_{i=1}^n -d_i \right]$$

A graph of total downthrow (fig. 12, center) indicates that most displacement took place in the zones of parallel faulting (up to 600 m offset at the base of the Austin Chalk), rather than in the intervening en echelon zone (traverse lines 5 and 6). These cumulative

<sup>1</sup>Dennis and Kelley (1980) emphasized the original concept of antithetic and synthetic structures (Cloos, 1928) as forming by small-scale movements that reduce or increase, respectively, relief of large-scale coeval structures. They also suggested using "homothetic" (after Lotze, 1931) rather than "synthetic" to avoid ambiguity. Other common definitions of synthetic and antithetic structures are of negligible use to structural geologists.

HORIZON I (86 Ma)  
MEXIA - TALCO FAULT ZONE

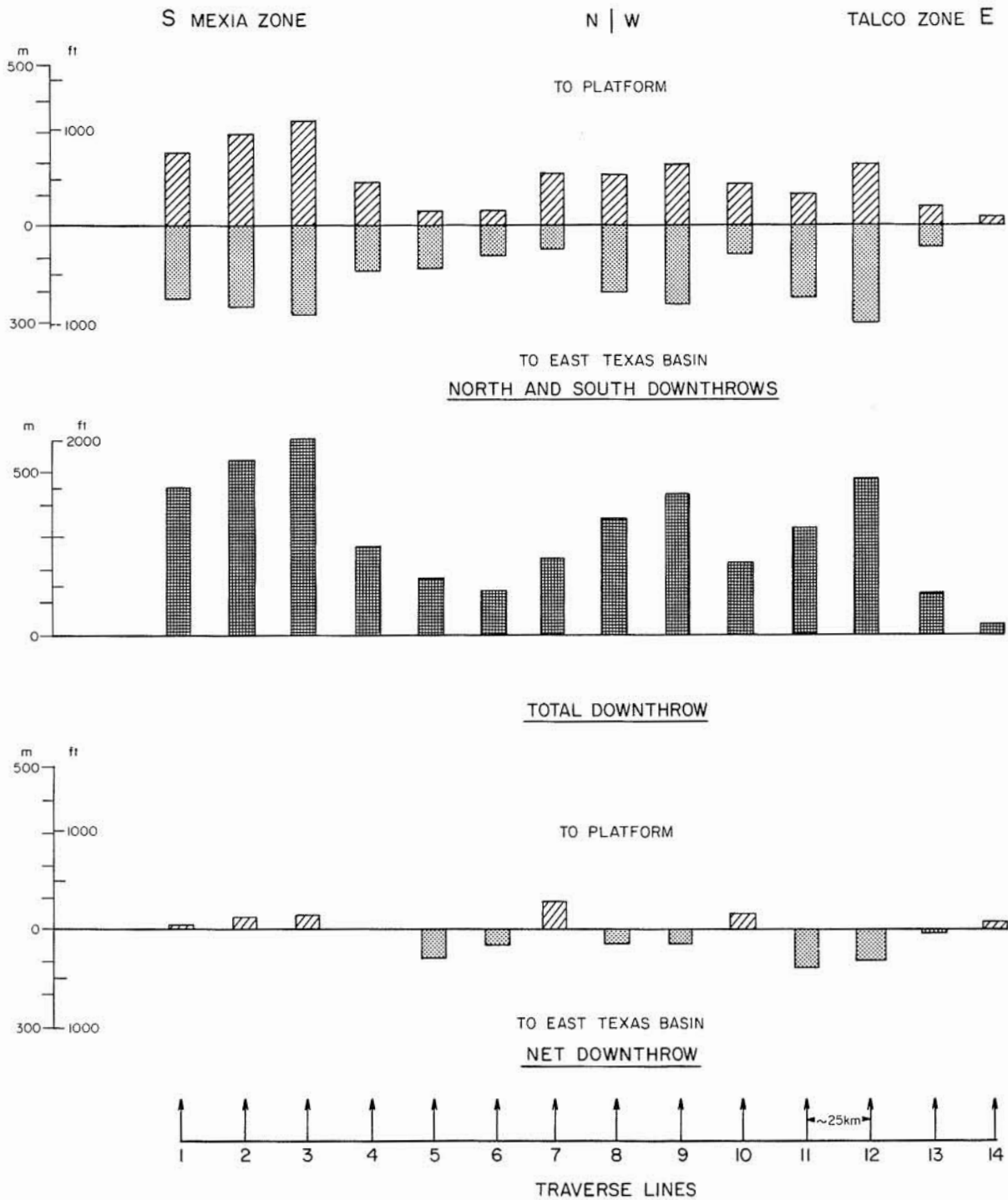


Figure 12. Bar graphs of throws inferred from structure-contour maps of the Mexia-Talco Fault Zone. Traverse lines (see fig. 7 for location) are oriented parallel to dip slip and are roughly equally spaced. Total downthrow refers to sum of absolute throws recorded along each traverse line. North and south downthrows refer to sum of downthrows toward platform and East Texas Basin, respectively, along each traverse line. Net downthrow represents the difference between north and south downthrows along each traverse line. See text for mathematical definitions. Data from GEOMAP Company (1980).

throws along each traverse line can be resolved into south downthrows toward the basin and north downthrows toward the platform (fig. 12, top). Balance between downthrows in these opposing directions is indicated by the relatively low net downthrows (fig. 12, bottom), thus confirming the symmetry of the peripheral graben throughout its length.

The Mexia-Talco faults were active from the Jurassic (and possibly the Triassic) until at least the Eocene--the youngest offset strata exposed. According to Turk, Kehle and Associates (1978), Quaternary terraces across these faults have not been offset, indicating that faulting ended during the Tertiary.

Certain hypotheses on the origin of the Mexia-Talco Fault Zone are considered untenable. The lack of evidence of underlying basement faults, apart from a possible connection with Triassic rift faults observed in one seismic line, suggests that differential movement in pre-Mesozoic crust is not a likely cause of the fault zone. Similarly, negligible flexure of pre- or post-Louann strata in the three seismic lines examined precludes crestal rupturing along a hypothetical hinge line at the basin margin (proposed by Colle and others, 1952, and Turke, Kehle and Associates, 1978) as a cause of faulting.

Although the graben system is symmetrical, the pronounced and uniform centripetal stratal dips indicate that the extension direction must have been downdip toward the center of the basin. Symmetrical grabens produced experimentally by downslope creep of clay have been modeled by Cloos (1968). In Cloos's model, grabens formed at the junction between a stable slab and one creeping laterally, and within the moving slab itself. The symmetrical graben in the clay model closely resembles that in the Mexia-Talco Fault Zone (compare figs. 11 and 13). Near coincidence between the updip limit of the Louann Salt and the graben system suggests that the highly mobile evaporites provided a weak décollement layer over which the overburden slowly glided toward the center of the basin. This hypothesis was also supported by Crosby (1971) on the basis of a gravity profile across the junction of the Mexia and Talco Fault Zones. He estimated minimum stratal extension of 0.5 km on the basis of summation of fault heaves and calculated elastic expansion just before faulting. Bishop (1973) inferred a similar process of stratal extension over a salt décollement in Louisiana and Arkansas. Updip of the Louann Salt subcrop in East Texas no such lubricating layer exists, and movement of the overburden was restricted; as a result of this differential movement of the post-Louann section, rupture and collapse occurred at the edge of the salt basin.

The high mobility of the Louann Salt, even where relatively thin and at shallow depths, is indicated by the growth of salt pillows during the Late Jurassic (fig. 10, seismic unit M3). The anomalously thin basal interval within the graben may have formerly contained post-Louann evaporites that were squeezed basinward because of the extra

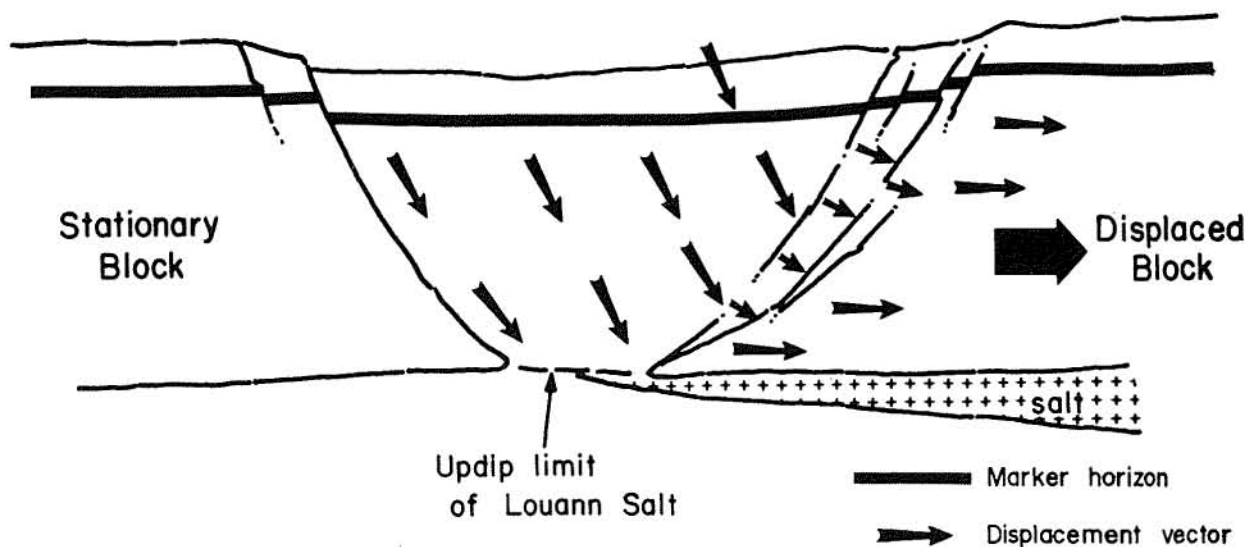


Figure 13. Conceptual diagram of a symmetric graben formed by asymmetric extension toward right due to gravitational sliding of displaced block over a décollement zone of weak Louann Salt. Graben structure and displacement vectors based on experimental model by Cloos (1968).

loading beneath the thick graben fill. The geometry of the Mexia-Talco Fault Zone suggests that the graben formed as a pull-apart structure between autochthonous salt-free strata and para-allochthonous strata underlain by mobile salt. Relative ductility and low shear strength of the salt allowed décollement and basinward creep of the overlying strata; the amount of salt creep is difficult to estimate, and it is possible that the Louann Salt originally extended farther updip than its present limits.

### FAULTS IN THE CENTRAL BASIN

Parallel normal faults in the deep subsurface are abundant in the salt-pillow province and the salt-diapir province of the East Texas Basin. These faults closely correspond spatially to the salt-related structures. In the deep Jurassic intervals (fig. 8) these faults form grabens more than 100 km long, parallel to the Mexia-Talco Fault Zone and to the trend of the peripheral salt pillows and related turtle structures that the faults overlie. At the Cretaceous horizons (figs. 6 and 7) these faults are concentrated over larger salt-related anticlines in the center of the basin that have affected higher stratigraphic levels because of their greater size. The faults are particularly abundant in the rim anticline surrounding the Hainesville rim syncline (Wood County, figs. 6 and 7). Few major subsurface faults occur above the salt diapirs because the diapirs are relatively small and are located in regional synclines.

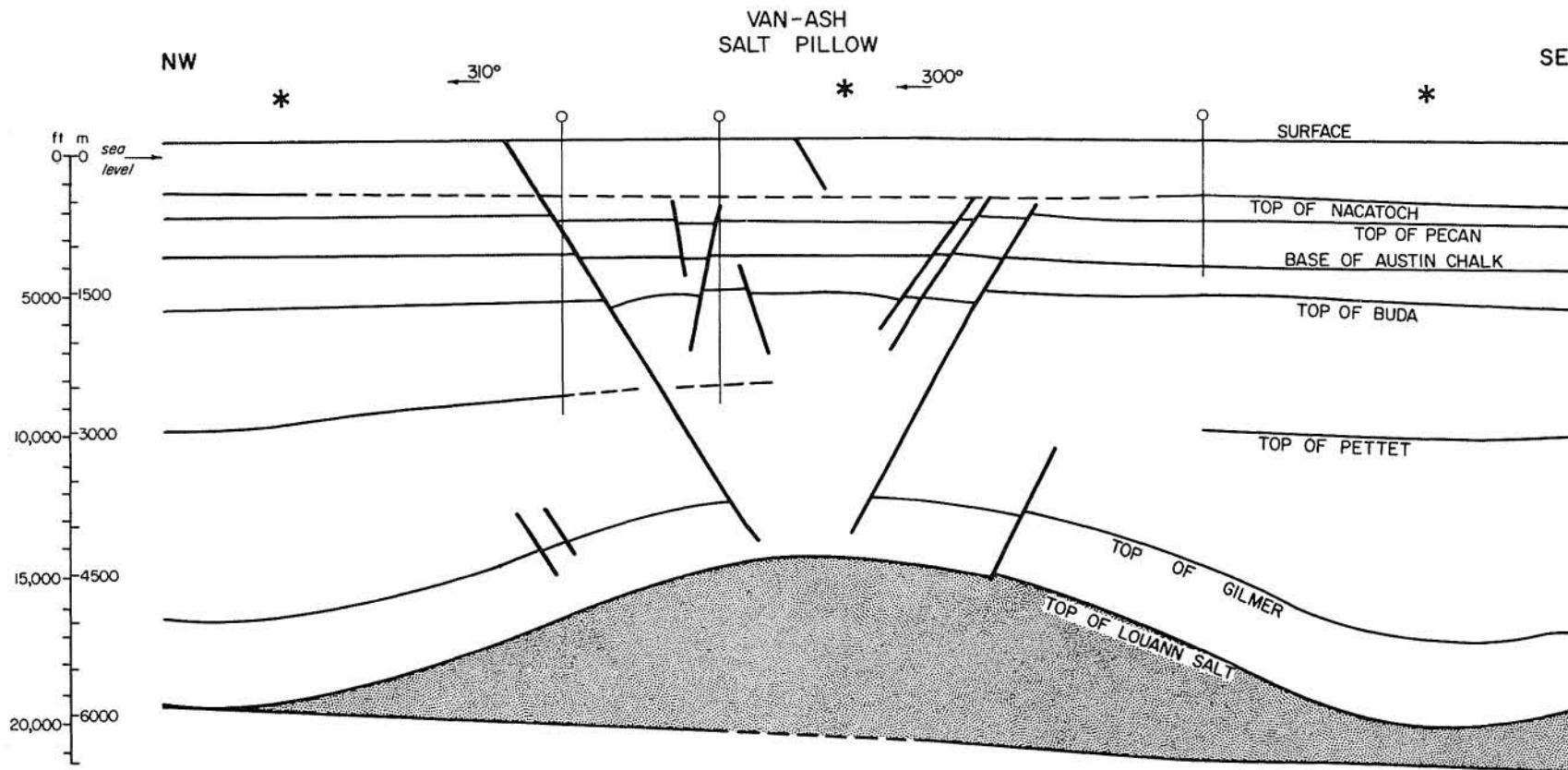
The localization of the central-basin faults on the crests of anticlinal structures such as salt pillows and turtle structures and the orientation of these faults parallel to the hinge lines of the anticlines indicate that the crests of these structures split by folding-related extension. All these normal faults are antithetic (Dennis and Kelley, 1980), in that they reduce structural relief (fig. 14). This antithesis indicates that the faults formed by crestal stretching and collapse rather than by the upward force of mobile core material such as salt or shale. Folding therefore took place predominantly by stretching of the outer fold arcs (tangential longitudinal strain [Ramsay, 1967]) rather than by flexural slip or shear folding. The central-basin faults are scarce at the surface (fig. 5), where folding is minimal (fig. 3).

In the deep Jurassic horizons (fig. 8), central-basin faults have also formed over the crests of anticlinal structures such as salt pillows and turtle structures in Wood, Rains, and Van Zandt Counties on the northwest flank of the basin. These faults arc southward, maintaining parallelism with the regional strike and the Mexia-Talco Fault Zone. Seismic reflection profiles indicate that this discontinuous zone of deeply buried, low-relief grabens follows the approximate subsurface boundary between undeformed salt and low-amplitude salt pillows (Jackson and Harris, 1981; Jackson and others, 1982). The paucity of faults on the map of the deep Jurassic horizons in the center of the basin (fig. 8) largely results from the absence of sufficiently deep holes. But this scarcity may also reflect the basinward migration of tectonic activity during the Late Jurassic, which has been inferred from the stratigraphic relations of salt structures in seismic reflection profiles (Jackson and others, 1982).

### ELKHART GRABEN

The Elkhart Graben constitutes the western end of the Elkhart-Mount Enterprise Fault Zone (fig. 15, southern end of traverse lines 1-4). It consists of parallel, normal faults with multiple offsets defining a graben approximately 40 km long. The graben resembles the central-basin faults more than it resembles the Mount Enterprise Fault Zone. The graben forms the southern component of a fan of central-basin faults trending toward Oakwood Dome on the southwest margin of the basin (fig. 15). Like these faults the Elkhart Graben overlies broad anticlinal structures, in this case salt pillows, and is parallel to the trend of these structures.

Throws along traverse lines 1 through 4 (fig. 15) across the Elkhart Graben and spatially related to central-basin faults are summarized in figures 16 and 17 for the Austin Chalk and Glen Rose horizons, respectively. Comparison of the graphs of total



Vertical scale = horizontal scale

- EXPLANATION**
- Reflector
  - - - Uncertain reflector
  - - - Fault trace
  - Well providing depth control
  - \* Seismic depth control
  - ▨ Louann Salt



**Errors in reflector depths**

- Nacatoch ± 90m (300ft)
- Pecan Gap ± 90m (300ft)
- Austin Chalk ± 90m (300ft)
- Buda ± 90m (300ft)
- Pettet ± 120m (400ft)
- Gilmer ± 180m (600ft)
- Louann ± 180m (600ft)

Fault traces projected to surface on the basis of Barnes (1965)  
 Seismic picks by D.W. Harris and C.D. Winker  
 Time-to-depth conversion by R.E. Anderson and T.E. Ewing based on electric logs and seismic velocity analyses

**Figure 14.** Time-to-depth converted seismic section across the junction of Van and Ash Salt Pillows showing symmetric buried graben over the crest of the pillow. Successively younger faults form progressively farther within the graben over the zone of maximum tension. All the faults are antithetic, indicating an origin by extension and collapse of strata.



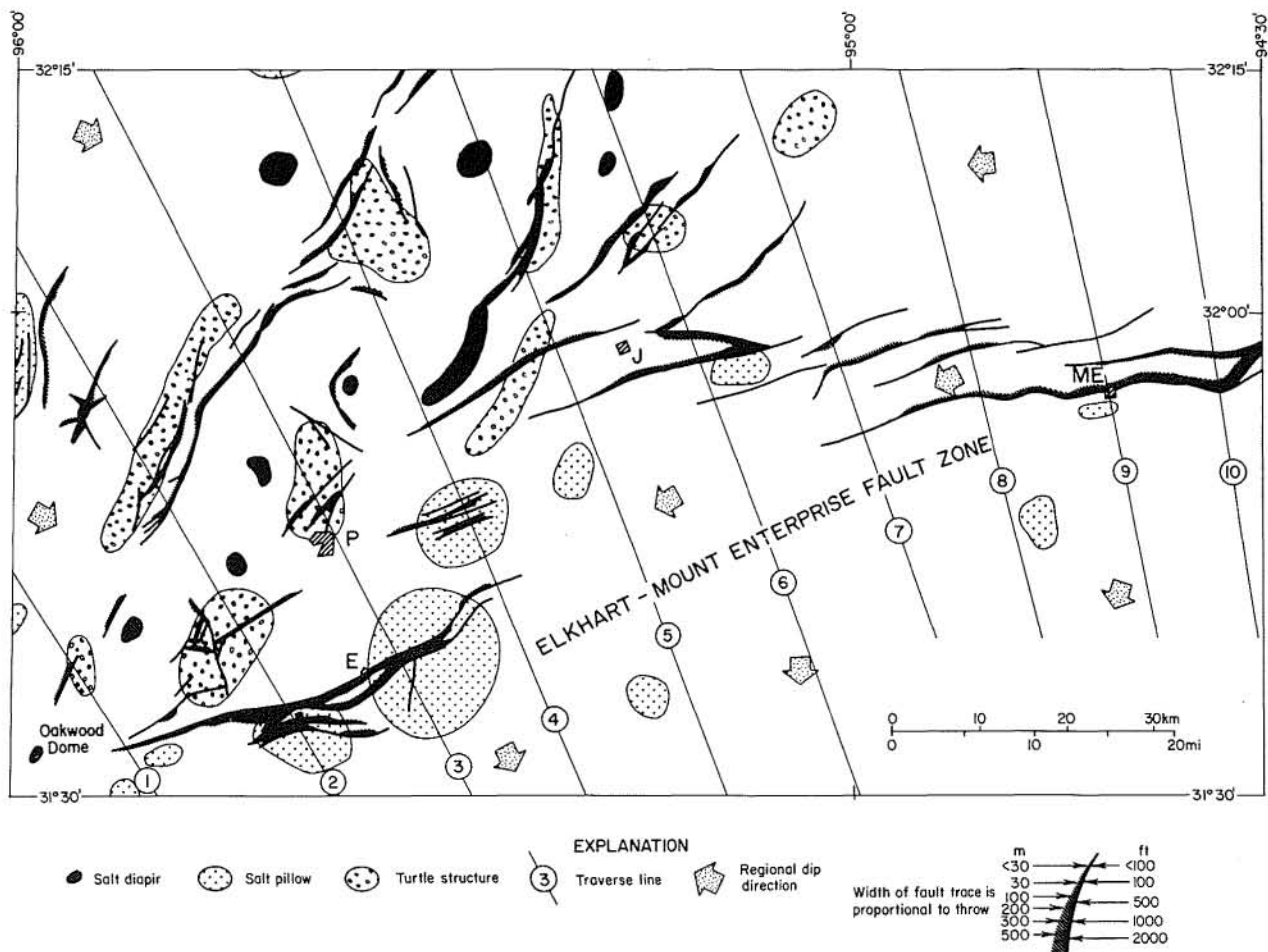


Figure 15. Map of fault traces of Elkhart-Mount Enterprise Fault Zone on horizon 2 showing relation to salt pillows, turtle structures, regional dip, and adjacent faults. Apart from the Mount Enterprise Fault Zone, the faults tend to be located over salt-related anticlines. Fault traces from GEOMAP Company (1980); distribution of salt structures adapted from Wood (1981). E=Elkhart; J=Jacksonville; ME=Mount Enterprise; P=Palestine.

downthrows shows that most of the displacement took place in the Early Cretaceous. Directions of net downthrows vary in both space and time: traverse lines 1 and 2 indicate net downthrow to the south affecting horizon 2 (Glen Rose), whereas traverse lines 3 and 4 show net downthrow to the north (fig. 16); furthermore, faults along traverse line 3 show net downthrow to the south on horizon 1 and to the north on horizon 2 (compare figs. 16 and 17). However, because these traverse lines include information from the central basin as well as the Elkhart Graben itself, these variations apply to an array of faults rather than to an individual fault.

The origin deduced for the central-basin faults on the basis of fault geometry also applies to the Elkhart Graben. Additional stratal extension could have been caused by the Angelina Flexure, a few kilometers south of the graben. The age of the youngest formation affected by faulting within the Elkhart Graben, the Eocene Cook Mountain

HORIZON 1 (36 Ma)  
ELKHART-MT. ENTERPRISE FAULT ZONE

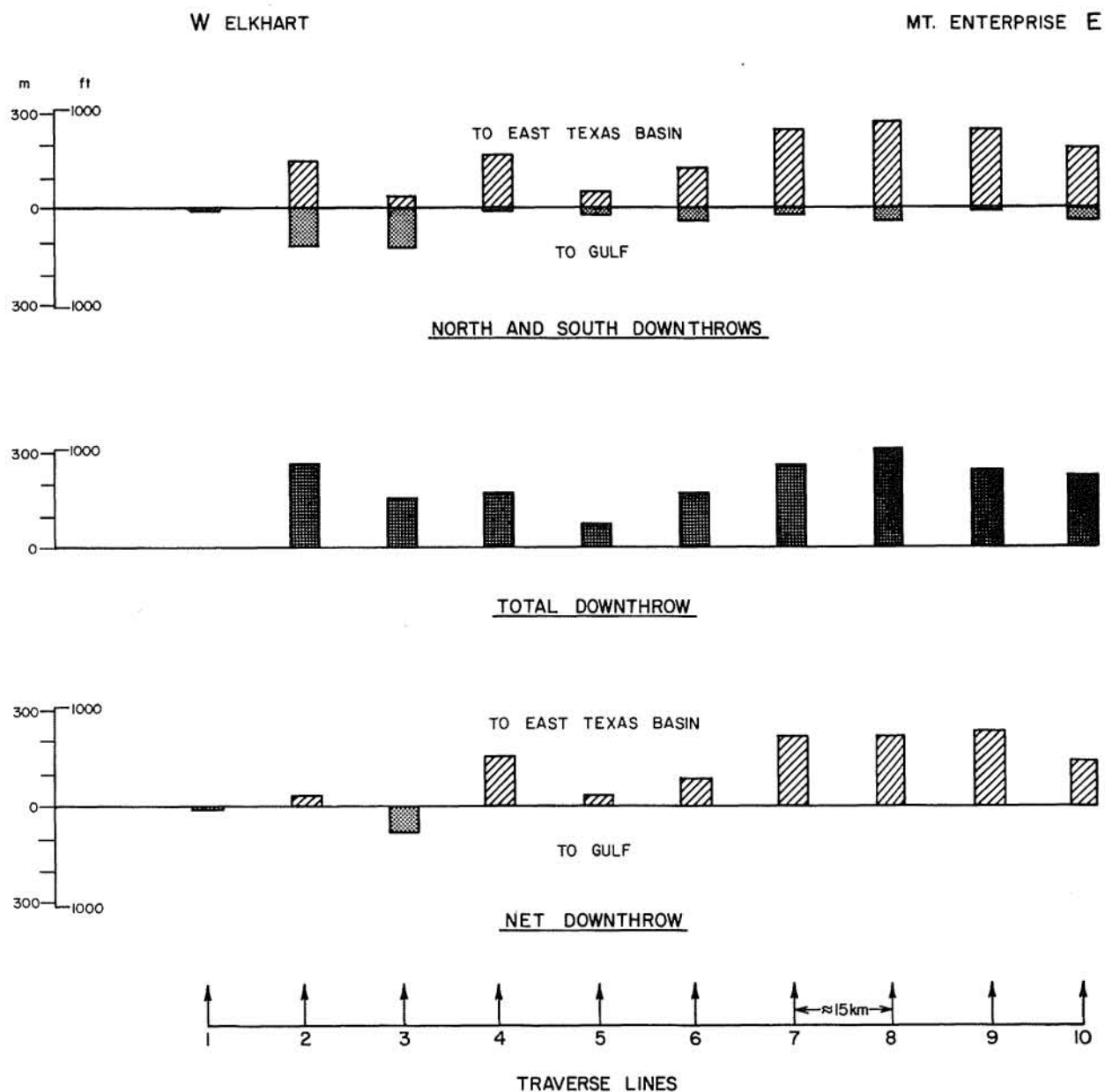


Figure 16. Bar graphs of throws of the Elkhart-Mount Enterprise Fault Zone inferred from structure contour maps on horizon 1. Traverse lines (see fig. 7 or 14 for location) are oriented parallel to dip slip and are roughly equally spaced. Total downthrow refers to sum of absolute throws recorded along each traverse line. North and south downthrows refer to sum of downthrows toward East Texas Basin and Gulf, respectively, along each traverse line. See text for mathematical definitions. Data from GEOMAP Company (1980).

HORIZON 2 (107/117 Ma)  
ELKHART-MT. ENTERPRISE FAULT ZONE

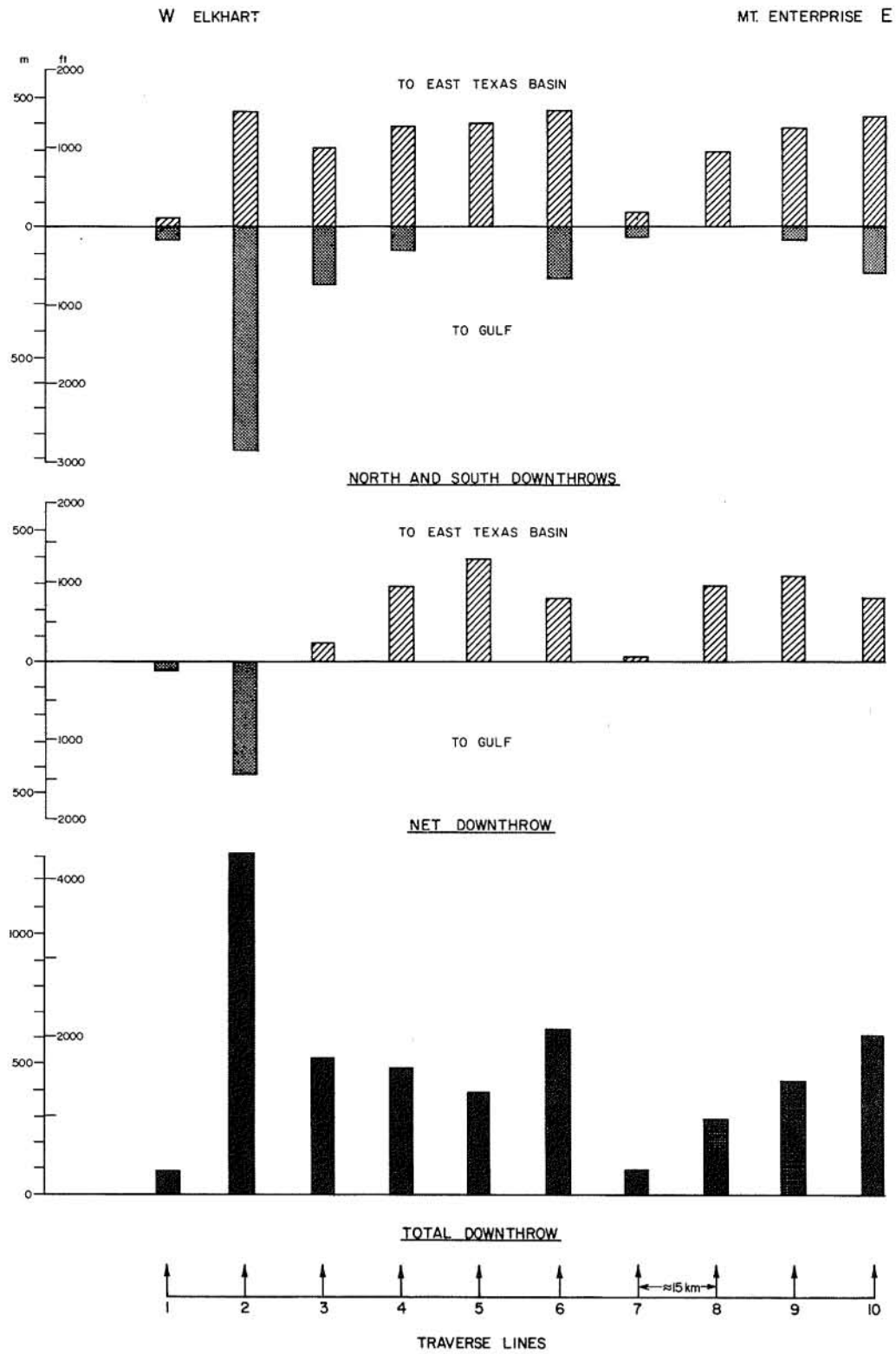


Figure 17. Bar graphs of throws of the Elkhart-Mount Enterprise Fault Zone inferred from structure-contour maps on horizon 2. Refer to figure 15 for explanation of terms and data source.

Formation, is approximately 40 Ma. Collins and others (1980) described normal faults exposed in the Trinity River along strike of the northern flank of the Elkhart Graben. Here a maximum throw of 66 cm was recorded in the Eocene Claiborne Group. These faults also offset the base of Quaternary terraces in the same exposure, which implies that faulting with small throws of about 5 cm took place as recently as 37,000 years ago.

### MOUNT ENTERPRISE FAULT ZONE

The Mount Enterprise Fault Zone lies east-northeast of the Elkhart Graben and is crossed by traverse lines 5 through 10 (fig. 15). The fault zone is a regular array of parallel and en echelon normal faults; the faults are largely downthrown to the north in a series of multiple offsets. The Mount Enterprise Fault itself forms the largest and southernmost component of the fault zone.

Unlike the other fault systems described in this report, the Mount Enterprise Fault Zone is not obviously connected to salt-related structures or to other basinal elements; the faults do not overlie salt pillows, turtle structures, or subcrop limits of Louann Salt, nor do they coincide with marginal flexures of the basin, such as the Angelina Flexure. Although the Mount Enterprise Fault Zone extends to the Sabine Arch, it shows no geometric relation to inferred flexure, gravitational spreading, or gliding possibly associated with growth of this arch.

The displacement history of this fault zone does not reveal its origin. The eastern and western ends of the fault zone were most active between 120 and 40 Ma, whereas the central parts were more active since 40 Ma (compare total downthrows in figures 16 and 17). At least some of this displacement was syndepositional with respect to the Paleocene-Eocene Wilcox Group, which shows approximately 10 percent overthickening in a central graben as well as a general gulfward increase in thickness (Wood and Guevara, 1981). Net downthrows on horizons 1 and 2 and at the surface show the strong dominance of northward downthrows on every traverse line crossing the Mount Enterprise Fault Zone. However, northward downthrow is not prevalent in the area immediately south of the fault zone. Here small faults show the down-to-the-south movement typical of the Gulf Coast faults. The Wilcox Group is approximately 100 m thicker on the southern side of some of these faults, and a releveling profile indicates a southern downthrow of 130 mm in 30 years (Collins and others, 1980).

A time-to-depth converted seismic profile across one of the major faults in the western part of the Mount Enterprise Fault Zone indicates the geometry of a large growth fault (fig. 18). This listric normal fault dips northward at  $75^{\circ}$  at the surface and at about

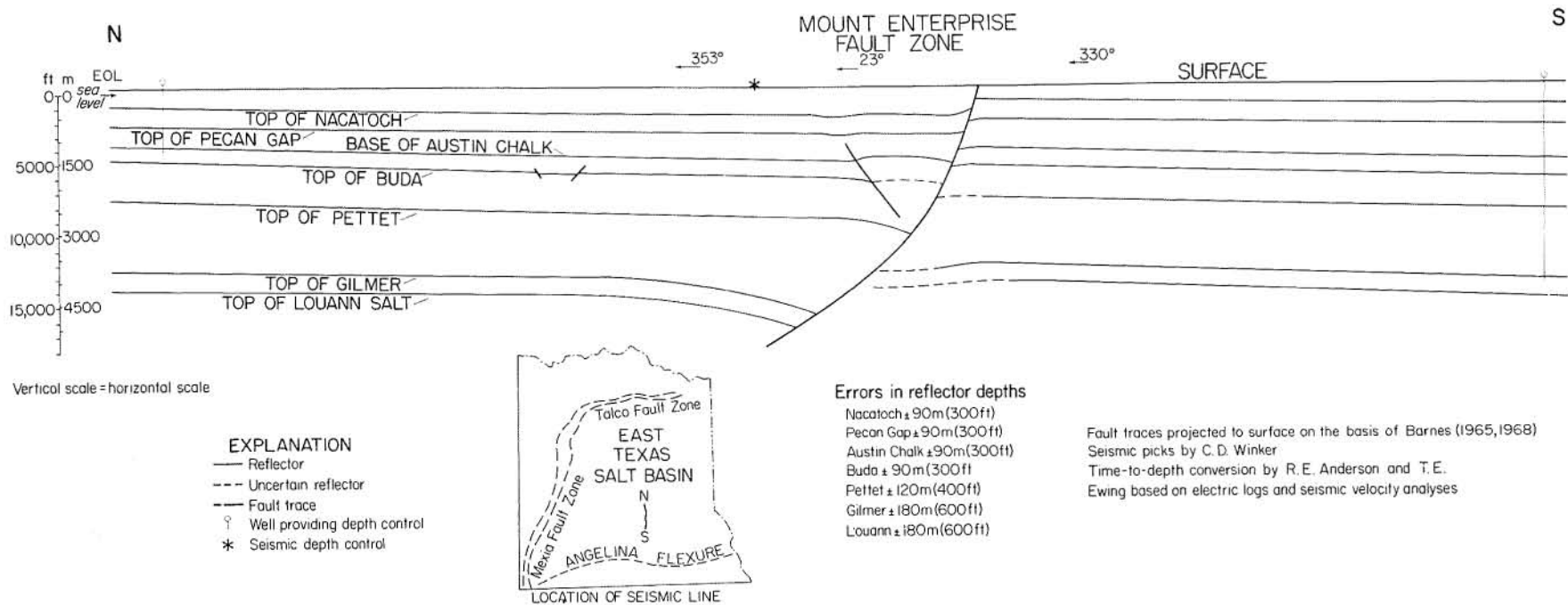


**Figure 18.** Time-to-depth converted seismic section across the central part of the Mount Enterprise Fault Zone. A large growth fault downthrown to the north and based in Louann Salt shows listric-normal geometry, decreasing cumulative displacement with time, and a rollover anticline on the northern hanging wall.

30° at depth, at which point it soles out into the Louann Salt. A rollover anticline and small antithetic fault have formed in the hanging wall block. Displacement increases from approximately 220 m on the top of the Nacatoch Formation near surface to 1,600 m on the top of the deep Gilmer Formation. Considerable thickening on the downthrown side is present throughout the Lower Cretaceous interval. Farther west, the near-surface geometry is similar although the deep structure is not clearly defined by seismic reflection (fig. 19).

Despite its many geometric similarities to the Gulf Coast growth faults, the Mount Enterprise growth fault differs in one important respect: it is downthrown to the north, facing the direction of terrigenous sediment supply. Little is known of the paleomorphology of the southern part of the East Texas Basin during Cotton Valley-Hosston times. Nevertheless, sand-distribution maps indicate that this interval accumulated by means of rivers flowing southeastward across the western flank of the basin. The fault zone area corresponded to the distal part of this alluvial plain, evolving into a delta plain toward the end of Hosston time (Bushaw, 1968). An open sea lay to the south of the fault zone, indicating that the paleoslope was southward at this stage. At the start of Glen Rose time this paleoslope was maintained, but transgression created shallow-marine environments over the fault zone and a beach zone to the northwest (Bushaw, 1968). In James time (early Glen Rose) the paleoslope had reversed so that deep open-shelf conditions prevailed near the fault zone, and shallow open-shelf conditions to the north and south; elevation of the southern area could have been tectonically induced (later manifested as the Angelina Flexure) or could have been caused by the continued growth of reefs south of the fault zone. By middle Glen Rose time, the fault zone was once again a shallow-marine environment of deposition (Bushaw, 1968).

On the basis of these inferred sedimentary environments, we deduce that the provenance lay north of the Mount Enterprise Fault Zone throughout the period of maximum displacement, as was the case for subsequent sedimentation; this deduction also applies to the later geologic history. The regional paleoslope was generally southward except during a comparatively short period in early Glen Rose time. Had sedimentary loading been the cause of growth faulting, these faults would have faced southward and been downthrown in the same direction; loading is therefore unlikely to have initiated faulting. Because there is no evidence of regional flexure at this location, flexure is also untenable as a means of initiating faulting. The growth fault flattens into the Louann Salt, indicating that extension resulted from relative northward movement of the post-Louann strata over a décollement zone of ductile salt. Northward thickening of Louann Salt combined with northward slope of the Jurassic basin margin may have caused the

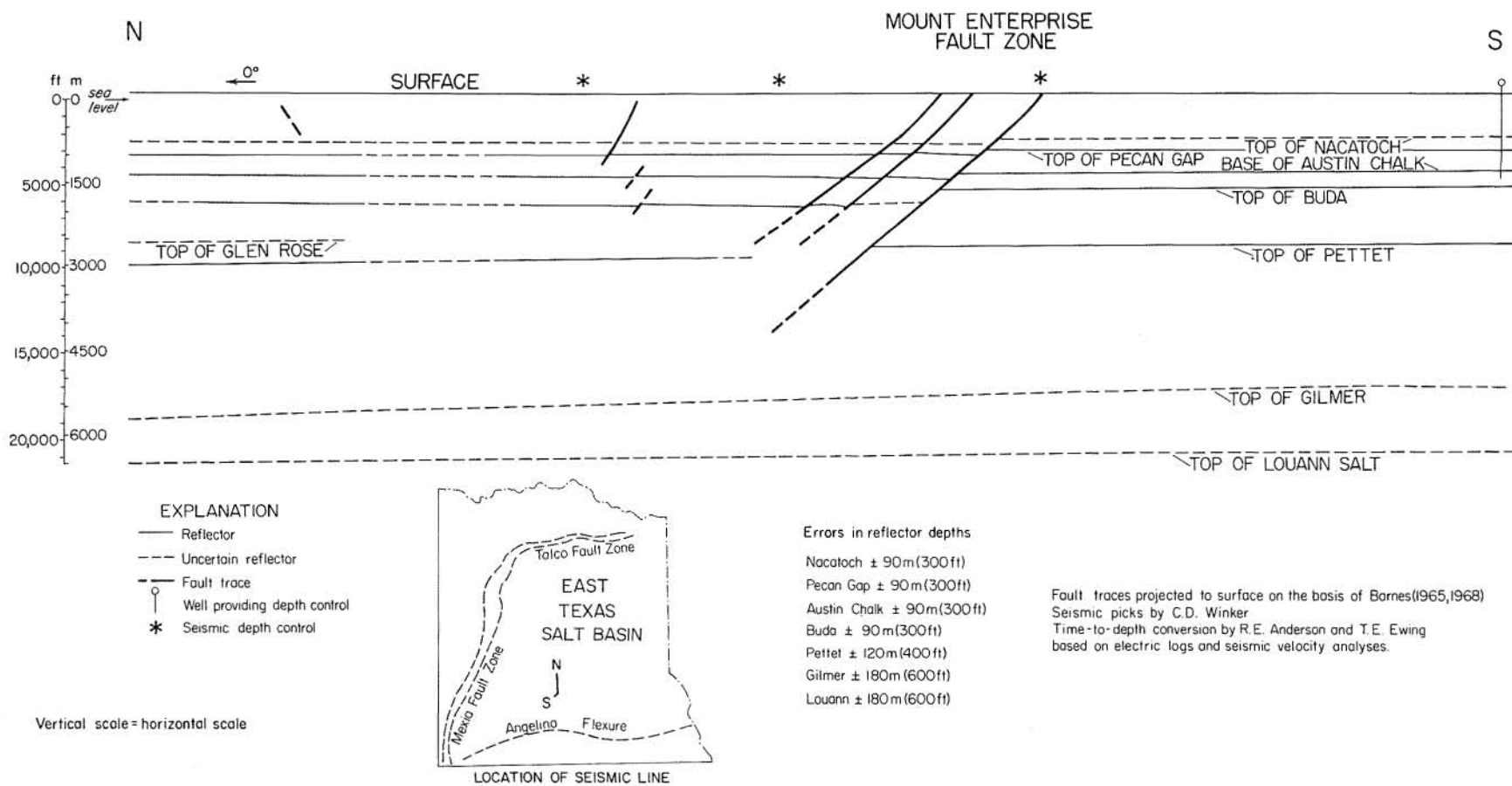


Figure 19. Time-to-depth converted seismic section across the western part of the Mount Enterprise Fault Zone. Multiple offsets show downthrow to the north. Weak reflectors at depth obscure the deep geometry of the fault zone, but the shallow parts are similar to those of figure 18.

thicker salt to flow faster than the thinner salt updip (compare Kehle, 1970). The zone of abrupt salt thickening would have been under tension because of these differential velocities. Strata above this zone would have undergone normal faulting as a result, thereby initiating subsidence and growth faulting. A submarine scarp was continuously smothered, and the downdropping proximal side acted as a subsiding trap for southward prograding terrigenous clastic material, even when the slope of the basin margin had reversed southward by Smackover time. Thicker deposits of carbonates would also have accumulated on the downthrown side because of its faster subsidence. Whatever the original triggering mechanism, this extra loading by the overburden--aided by a tensile stress regime near the basin margin--would have tended to perpetuate subsidence in the manner of all growth faults.

Because the original cause of the Mount Enterprise Fault Zone is uncertain, the possibility of basement control has not been disproven. Nevertheless available evidence indicates that these faults result from long-continued extension and differential subsidence in the Louann and post-Louann strata.

#### SEISMIC POTENTIAL OF EAST TEXAS FAULTS

East Texas faults share numerous indicators of low seismic risk. Normal displacements ensure that stresses are neutralized by tensile fracture at low stresses because the tensile strength of materials is generally much lower than their compressive strength. Furthermore, almost all these faults are related to slow gravitational creep of salt and its sedimentary overburden rather than to movement of lithospheric plates. Moreover, future movement on the Mexia-Talco Fault Zone is extremely unlikely because undeformed Pleistocene terraces cross them (Turk, Kehle and Associates, 1978). Similarly, only a few central-basin faults extend upward to the Lower Tertiary stratigraphic units exposed at the surface.

The Mount Enterprise Fault Zone is the least understood zone in East Texas because of poor subsurface information. At least one seismic profile indicates that it, like the Mexia-Talco Fault Zone, is based in the Louann Salt, which suggests that the Mount Enterprise Fault Zone is also related to salt creep, indicating a low seismic potential. Nevertheless, a compelling reason for detailed study of the Mount Enterprise Fault Zone is the prevalence of microseismic tremors in this area, a notable example being the Jacksonville earthquake of November 6, 1981, which had a Richter intensity of 3.5 to 4.0. Microseismic activity in the East Texas Basin is currently being monitored (Pennington and others, 1981).



## CONCLUSIONS

The Mexia-Talco Fault Zone formed as a pull-apart structure between autochthonous salt-free strata and para-allochthonous strata underlain by mobile salt that allowed overburden creep into the East Texas Basin.

The Elkhart Graben and the central-basin faults formed by crestal stretching and collapse of salt-related anticlines such as salt pillows and turtle structures.

At least one western fault in the Mount Enterprise Fault Zone is a long-active listric normal growth fault, downthrown to the north and based in the Louann Salt. Its origin is obscure. Once initiated, its growth would have been perpetuated by loading induced by sediments trapped on the downthrown side and by the tensile stress regime near the basin margins.

All the faults studied (1) are normal, (2) moved steadily during the Mesozoic and Early Tertiary, and (3) appear to be related to salt mobilization. Faulting ceased before the Quaternary except for a westward extension of the north flank of the Elkhart Graben and small faults south of the Mount Enterprise Fault Zone.

No geologic evidence indicates that any of these faults poses a seismic threat to a hypothetical nuclear-waste repository. In the case of the Mount Enterprise Fault Zone, however, available meager information suggests that this structure is sufficiently unusual to warrant direct study of its current activity by microseismic monitoring.

## ACKNOWLEDGMENTS

This work was funded by the U.S. Department of Energy under contract number DE-AC97-80ET-46617. We thank T. E. Ewing, A. G. Goldstein, and S. J. Seni for reviewing this paper. R. G. Anderson, T. E. Ewing, D. W. Harris, and C. D. Winker assisted by interpreting seismic reflection profiles and converting these to depth sections. Figures were drafted by John T. Ames, Margaret R. Day, Margaret L. Evans, Byron P. Holbert, Jeffrey Horowitz, and Jamie McClelland, under the supervision of Dan F. Scranton. Photographic printing was by James A. Morgan. Word processing was by Dottie Johnson. This publication was edited by Amanda R. Masterson and designed and assembled by Micheline Davis.

## REFERENCES

- Barnes, V. E., 1965, Tyler sheet: University of Texas, Austin, Bureau of Economic Geology, Geologic Atlas of Texas, scale 1:250,000.
- \_\_\_\_\_ 1966, Texarkana sheet: University of Texas, Austin, Bureau of Economic Geology, Geologic Atlas of Texas, scale 1:250,000.
- \_\_\_\_\_ 1967, Sherman sheet: The University of Texas at Austin, Bureau of Economic Geology, Geologic Atlas of Texas, scale 1:250,000.
- \_\_\_\_\_ 1968, Palestine sheet: The University of Texas at Austin, Bureau of Economic Geology, Geologic Atlas of Texas, scale 1:250,000.
- \_\_\_\_\_ 1970, Waco sheet: The University of Texas at Austin, Bureau of Economic Geology, Geologic Atlas of Texas, scale 1:250,000.
- \_\_\_\_\_ 1972, Dallas sheet: The University of Texas at Austin, Bureau of Economic Geology, Geologic Atlas of Texas, scale 1:250,000.
- Bishop, W. F., 1973, Late Jurassic contemporaneous faults in north Louisiana and south Arkansas: American Association of Petroleum Geologists Bulletin, v. 57, no. 5, p. 858-877.
- Bushaw, D. J., 1968, Environmental synthesis of the East Texas Lower Cretaceous: Gulf Coast Association of Geological Societies Transactions, v. 18, p. 416-438.
- Cloos, H., 1928, Uber antithetische Bewegungen: Geologische Rundschau, v. 19, no. 3, p. 246-251.
- \_\_\_\_\_ 1968, Experimental analysis of Gulf Coast fracture patterns: American Association of Petroleum Geologists Bulletin, v. 52, no. 3, p. 420-444.
- Colle, J., Cooke, W. F., Jr., Denham, R. L., Ferguson, H. C., McGuirt, J. H., Reedy, F., Jr., and Weaver, P., 1952, Part IV: Volume of Mesozoic and Cenozoic sediments in western Gulf Coastal Plain of United States and Mexico: Geological Society of America Bulletin, v. 63, no. 12, p. 1193-1199.
- Collins, E. W., Hobday, D. K., and Kreitler, C. W., 1980, Quaternary faulting in East Texas: The University of Texas at Austin, Bureau of Economic Geology Geological Circular 80-1, 20 p.
- Crosby, G. W., 1971, Gravity and mechanical study of the Great Bend in the Mexia-Talco fault zone, Texas: Journal of Geophysical Research, v. 76, no. 11, p. 2690-2705.

- Dennis, J. G., and Kelley, V. C., 1980, Antithetic and homothetic faults: *Geologische Rundschau*, v. 69, no. 1, p. 186-193.
- GEOMAP Company, 1980, *Geologic Atlas of East Texas*: Dallas, GEOMAP, scale 1:48,000.
- Jackson, M. P. A., and Harris, D. W., 1981, Seismic stratigraphy and salt mobilization along the northwestern margin of the East Texas Basin, *in* Kreitler, C. W., and others, *Geology and geohydrology of the East Texas Basin: a report on the progress of nuclear waste isolation feasibility studies (1980)*: The University of Texas at Austin, Bureau of Economic Geology Geological Circular 81-7, p. 28-32.
- Jackson, M. P. A., Seni, S. J., and McGowen, M. K., 1982, Initiation of salt flow in the East Texas Basin (abs.): *American Association of Petroleum Geologists Bulletin*, v. 66, no. 5, p. 584-585.
- Kehle, R. O., 1970, Analysis of gravity sliding and orogenic translation: *Geological Society of America Bulletin*, v. 81, no. 6, p. 1641-1663.
- Lotze, F., 1931, *Über Zerrungsformen*: *Geologische Rundschau*, v. 22, no. 6, p. 353-371.
- Martin, R. G., 1978, Northern and eastern Gulf of Mexico continental margin stratigraphic and structural framework, *in* Bouma, A. H., Moore, G. T., and Coleman, J. M., eds., *Framework, facies, and oil-trapping characteristics of the upper continental margin*: *American Association of Petroleum Geologists Studies in Geology No. 7*, p. 21-42.
- Pennington, W. D., Kreitler, C. W., and Collins, E. W., 1981, Seismicity near Rusk, East Texas: *Geological Society of America, Abstracts with Programs*, v. 13, no. 5, p. 260.
- Ramsay, J. G., 1967, *Folding and fracturing of rocks*: New York, McGraw-Hill, 568 p.
- Salvador, A., and Green, A. R., 1980, Opening of the Caribbean Tethys (origin and development of the Caribbean and the Gulf of Mexico), *in* *Colloque C5: Géologie des chaînes alpines issues de la Téthys*: Bureau de Recherches Géologiques et Minières, *Mémoire 115*, p. 224-229.
- Thomas, W. A., 1976, Evolution of Ouachita-Appalachian continental margin: *Journal of Geology*, v. 84, p. 323-342.
- Trusheim, F., 1960, Mechanism of salt migration in northern Germany: *American Association of Petroleum Geologists Bulletin*, v. 44, no. 9, p. 1519-1540.
- Turk, Kehle and Associates, 1978, *Tectonic framework and history, Gulf of Mexico region*: report prepared for Law Engineering Testing Co., Marietta, Georgia, 29 p.

Wood, D. H., 1981, Structural effects of salt movement in the East Texas Basin, in Kreitler, C. W., and others, Geology and geohydrology of the East Texas Basin: a report on the progress of nuclear waste isolation feasibility studies (1980): The University of Texas at Austin, Bureau of Economic Geology Geological Circular 81-7, p. 21-27.

Wood, D. H., and Guevara, E. H., 1981, Regional structural cross sections and general stratigraphy, East Texas Basin: The University of Texas at Austin, Bureau of Economic Geology Cross Sections.

